

PREPARATION AND CHARACTERIZATION OF CERAMIC MICROFILTRATION MEMBRANE USING RED MUD AS COST EFFECTIVE RESOURCE

Thesis Report of M.Tech Thesis



Submitted by

Sandeep Parma

211CH1255

Under the guidance of

Dr. Pradip Chowdhury

DEPARTMENT OF CHEMICAL ENGINEERING
NATIONAL INSTITUTE OF TECHNOLOGY ROURKELA

MAY 2013

National Institute Of Technology Rourkela

Department of Chemical Engineering



Certificate

This is to certify that the project report entitled, “**Preparation and Characterization of Ceramic Microfiltration Membrane using Red Mud as cost effective resource**” submitted by **Sandeep Parma** in partial fulfilments for the award of Master of Technology Degree in Chemical Engineering in National Institute of Technology, Rourkela is prepared under my supervision and guidance

Date:

Place:

Thesis Supervisor: _____

Dr. Pradip Chowdhury

Assistant Professor
Department of Chemical Engineering
National Institute of Technology
Rourkela

ACKNOWLEDGEMENTS

First and the foremost, I would like to offer my sincere thanks and gratitude to my thesis supervisor, **Dr. Pradip Chowdhury** for his immense interest and enthusiasm on the project. His technical prowess and vast knowledge on diverse fields left quite an impression on me. Although the journey was beset with complexities but I always found his helping hand when it mattered most. He has been a constant source of encouragement for me.

I am also thankful to all faculties and support staff of Department of Chemical Engineering, Department of Materials and Metallurgical Engineering and Department of Mechanical Engineering National Institute of Technology, Rourkela, for constant help and extending the departmental facilities for my project work.

I would like to extend my sincere thanks to my friend and colleague, Prasanna Rao Ravi for his unconditional encouragement, for the stimulating discussions, and also to my senior, Sankaranarayanan H for sincere help extended in completion of my project and for all the fun we have had in the last two years.

Last but not the least, I wish to profoundly acknowledge my parents for their constant support.

Sandeep Parma

(211CH1255)

ABSTRACT

This work highlights the fabrication of ceramic microfiltration membranes using *Red mud* as the raw material. The raw material was pre-processed and paste casting method was used for fabrication. Two different membranes were successfully fabricated: **membrane A** and **membrane B**. *Membrane A* had a regular stoichiometric composition of *red mud* and *binding agents* whereas in case of *membrane B*, a significant percentage of *kaolin* was added to prop up the membrane matrix. After initial treatments, both the membranes were sintered at high temperatures e.g. 800 and 900°C respectively. Comprehensive material characterization techniques viz. scanning electron microscopy (SEM), powder X-ray diffraction (PXRD), BET surface area analysis, Thermogravimetric analysis (TGA) and Mercury intrusion porosimetry were followed to ascertain the nature of the membrane fabrication and their inherent material properties.

The *membranes A* and *B* being sintered at 900°C, reported an average pore size of 10 and 6µm respectively. These membranes were found well suited for oil-water emulsion and clarifying raw sugar cane juice studies. A maximum rejection of 53% was achieved with *membrane B* in oil-water emulsion studies. In sugar cane juice study as well, *membrane B* performed superior to its counterpart. The performance was reasonably well and *membrane B* reported 78% of turbidity and 28% of colour removal. In addition to that purity percentage was increased to 1.7 units.

All the membranes were studied for their regeneration and reusability. The role of organic solvents was found to be important along with hot water wash. A detailed cost analysis was also performed and it was seen that the membranes fabricated were much cheaper than the similar products reported in literature.

TABLE OF CONTENTS

<i>Abstract</i>	<i>IV</i>
<i>List of Figures</i>	<i>VIII</i>
<i>List of Table</i>	<i>IX</i>
<i>List of Symbols</i>	<i>X</i>
CHAPTER 1: INTRODUCTION	1
1.1 Background of Present Research Work	1
1.2 Research Objectives	2
1.3 Thesis research objectives	3
CHAPTER 2: LITERATURE REVIEW	4
2.1 Red mud	4
2.1.1 Chemical composition	4
2.1.2 Uses of red mud	5
2.2 General theory and classification of membranes	5
2.2.1 Isotropic membrane	6
2.2.2 Anisotropic	6
2.2.3 Ceramic, metal, and liquid membrane	7
2.2.3.1 Ceramic membrane	8
2.3 Microfiltration of raw sugar cane juice	9
2.4 Ceramic MF/UF membranes for separation of crude-oil	10
2.5 Characterization technics	10

2.5.1 Scanning electron microscopy	10
2.5.2 X-ray Diffraction	11
2.5.3 BET Surface Area Analysis	13
2.5.4 Thermal gravimetric analysis	14
2.5.5 Mercury intrusion porosimetry	15
CHAPTER 3: EXPERIMENTAL WORKS	17
3.1 Introduction	17
3.2 Chemicals utilization and characterization	18
3.2.1 Chemicals	18
3.2.2 Membrane characterization	18
3.3 Fabrication of membrane	18
3.4 Permeation and filtration experiment	20
3.4.1 Design of filtration set up	20
3.4.2 Hydraulic permeability studies	22
3.4.3 Separation of crude oil from crude oil-water emulsion	23
3.4.3.1 Experimental protocol for feed preparation and estimation of Crude oil-water emulsion	23
3.4.3.2 Filtration experiment	24
3.4.3.3 Membrane recoverability	25
3.4.4 Clarifying of sugar cane juice	25
3.4.4.1 Experimental protocol for feed preparation and estimation of Sugar cane juice	25
3.4.4.2 Membrane recoverability	26

CHAPTER 4: RESULTS AND DISSCUSSION	27
4.1 Powder X-ray Diffraction	27
4.2 Scanning electron microscopy (SEM) analysis	29
4.3 Mercury porosimetry analysis of membranes	30
4.4 BET Surface area analysis	34
4.5 Thermo gravimetric analysis	35
4.6 Permeation experiment	36
4.7 Separation experiment	37
4.7.1 Microfiltration of Sugar cane juice	37
4.7.2 Separation of crude oil from crude oil-water emulsion	41
4.8 Estimation of material cost of the membrane	43
CHAPTER 5: CONCLUSIONS	44
CHAPTER 6: REFERENCES	45

LIST OF FIGURES

Figure no.	Figure caption	Page No.
Figure 3.1	Schematic diagram of experimental set up for permeation and separation studies	20
Figure 3.2	Side view and top view of membrane module experimental set up for permeation and separation studies	21
Figure 4.1	XRD Analysis of membrane A sintered at 800 ⁰ C and 900 ⁰ C	27
Figure 4.2	XRD Analysis of membrane B sintered at 800 ⁰ C and 900 ⁰ C	28
Figure 4.3	SEM Images of membrane A sintered at 800 ⁰ C and 900 ⁰ C	29
Figure 4.4	SEM Images of membrane B sintered at 800 ⁰ C and 900 ⁰ C	29
Figure 4.5	Multimodal pore size distribution of membrane A	30
Figure 4.6	Multimodal pore size distribution of membrane B	31
Figure 4.7	Pore size distribution of membrane A	32
Figure 4.8	Pore size distribution of membrane B	33
Figure 4.9	BET Isotherm of Red mud	34
Figure 4.10	TGA Pattern of membrane before sintering	35
Figure 4.11	Permeate Flux (de-ionized water)	37
Figure 4.12	Permeate flux of sugar cane juice at 300KPa of membrane A	39
Figure 4.13	Permeate flux of sugar cane juice at 300KPa of membrane B	40

LIST OF TABLES

Table no.	Table Caption	Page No.
Table 2.1	The main chemical constituents of red mud	4
Table 3.1	Composition of membrane A (without kaolin)	18
Table 3.2	Composition of membrane B (with kaolin)	19
Table 4.1	Composition of juice properties (permeate)	38
Table 4.2	Composition of juice properties at different flux at 300KPa of Membrane A	41
Table 4.3	Composition of juice properties at different flux at 300KPa of Membrane B	41
Table 4.4	Summary of crude oil – water emulsion separation using membrane B	42

LIST OF SYMBOLS

C_i	-	Concentration of solute in feed
C_f	-	Concentration of solute in permeate
R	-	Rejection of solute
K	-	Permeability
ΔP_h	-	Hydrostatic pressure difference across membrane
ΔP_i	-	Osmotic pressure difference
L	-	Membrane thickness
r_p	-	Mercury intrusion pore radius
γ	-	Surface tension of mercury
θ	-	Contact angle of mercury
V_{total}	-	Total pore volume (<i>Using Hg porosity analysis</i>)
$D_v (d)$	-	Volume pore size distribution
D_{eff}	-	Effective diffusivity
D_b	-	Bulk diffusivity
θ_c	-	Pore volume fraction
τ	-	Tortuosity factor
Lh	-	Hydraulic permeability
rl	-	Average pore radius (<i>Using hydraulic permeability studies</i>)
J	-	Liquid Flux across membrane
μ	-	Viscosity of water
P	-	Porosity
mD	-	Dry membrane support mass
mw	-	Mass of the support with pores filled with water
mA	-	Mass of the water saturated support measured in water

CHAPTER 1

INTRODUCTION

Here, the basics on membrane science and technology and the chronological developments over the years are highlighted. It is noteworthy to mention that the membrane science and technology is a modern unit operation which has been gaining in rapid strides over the last decade or so. And the application of membrane filtration for clarification of sugarcane juice and the removal oil from oil-water emulsion where studied.

1.1 Background of Present Research Work

The applications of ceramic membrane have increased due to its excellent chemical, thermal and mechanical stability and higher separation efficiency. In near future, the emergence of new type of ceramic materials and simple fabrication techniques may lead to preparation of low cost membranes. The applications of alumina-based ceramic membranes are limited due to higher cost and sintering temperature during fabrication. Therefore, the natural clay based low cost ceramic membranes would be an attractive proposition. Many researchers have already used low cost clays such as raw clay, moroccan clay, tunisian clay, sepiolite clay, algerian clay, dolomite and kaolin for membrane fabrication. Kaolin is one of the cheapest membrane raw materials easily available in India. Various researchers have reported the use of kaolin and natural clay as a starting material with other additives for membrane applications.

Red mud is a reddish brown colored solid waste produced during the physical and chemical processing of bauxite for the production of aluminium. Bauxite is composed of aluminum hydroxide minerals, primarily composed of gibbsite ($\text{Al}(\text{OH})_3$), boehmite ($\gamma\text{-AlO}(\text{OH})$), diaspor ($\alpha\text{-AlO}(\text{OH})$), hematite (Fe_2O_3) and goethite ($\text{FeO}(\text{OH})$). In this research work, effort has been given in utilizing a solid industrial effluent for gainful purpose.

A large quantity of oily wastewater is generated from various process industries: particularly from refineries and metallurgical plants. It is highly essential to separate the oily component before being discharged into a municipal sewage system to protect the environment by maintaining government regulations. Additionally, it might yield some value added product. Conventional methodologies like skimming, gravity settling etc. take longer time between

batches, requires large spaces and higher logistical supports. Membrane technology on the other hand follows a compact design and relatively low operational costs.

Similarly, the sugar industry needs to find efficient methods in clarifying the raw sugar cane juice, improve the quality of the clarified juice and to reduce or eliminate the usage of chemicals (lime). Conventional clarifiers use heavy equipment's which lead to high operating costs and associated environmental problems. In sugar mills, ensuring the production of juice of consistently high clarity and low color through the clarification process is a challenging task. The variations in the incoming juice characteristics due to differences in cane variety, soil and growing conditions, weather patterns and season makes this task even more challenging. The membrane filtration promises superior quality juice with better clarity, much lower viscosity and noticeable color removal.

1.2 Research objectives

The main objectives our present research work can be summarized as follows:

- (A) Preparation and characterization of ceramic membranes using red mud
- (B) Experimentally studying the performance of the fabricated membrane in separating crude oil from oil-water emulsion within the microfiltration regime
- (C) Studying the effectiveness of the membrane in clarification of raw sugarcane juice by removing colour ingredients
- (D) Detailed analysis on membrane fouling and regeneration
- (E) Cost analysis related to membrane fabrication and comparison with existing literature data on similar surfaces

1.3 Thesis Summary

This thesis comprises of five chapters *viz.* Introduction, Literature Review, Experimental Works, Results and Discussion and Conclusions. Each of these chapters adequately details about past and present research in similar fields, experimental methodologies followed, research findings and their possible explanations.

Chapter 1 introduces the field of research in brief, comprehensive description of research background, objectives of this work and thesis overview.

Chapter 2 discusses the literature reports in detail pertaining to field of ceramic membrane. Important methodologies on ceramic membrane fabrication and their important applications are also highlighted in detail. Various terminologies related to membranes especially on ceramic membranes are introduced and elaborated.

Chapter 3 describes the methodologies and protocols followed fabrication of ceramic membrane; preparation of clay based membrane and fabrication methodologies followed for membrane preparation. The step by step protocol for water permeation studies, filtration experiments for crude oil-water emulsion and clarification of raw sugarcane juice by removing colour ingredients also illustrated. The quantitative estimation techniques for permeate quality is also explained in detail using a series of mathematical equations.

Chapter 4 incorporates various results obtained during this study. The possible explanation of various observations is also given in detail.

Chapter 5 concludes the results and observation during this study. The major highlights of this work are also summarized.

Chapter 2

LITERATURE REVIEW

This chapter is dedicated entirely to discuss in detail the reported works by various research groups in the field of ceramic membrane and particularly focusing on the aspects of low cost ceramic membranes for the removal of crude oil from crude oil-water emulsion and to clarifying the raw sugar cane juice.

2.1 Red mud

Red mud is a reddish brown coloured solid waste produced during the physical and chemical processing of bauxite. Bauxite is composed of aluminum hydroxide minerals, including primarily gibbsite ($\text{Al}(\text{OH})_3$), boehmite ($\gamma\text{-AlO}(\text{OH})$), diaspor ($\alpha\text{-AlO}(\text{OH})$), hematite (Fe_2O_3) and goethite ($\text{FeO}(\text{OH})$) [1]. The red mud, according to the production process of the aluminum, can be divided into Bayer process red mud, sintering progress red mud, and combined process red mud. It was reported that there is 0.8~1.5 t of red mud produced by each 1 t alumina produced. Globally, the total amount of red mud produced every year is between 60 and 120 million tons. [1]

2.1.1 Chemical composition

There are different aluminium production processes to different bauxites. Red mud is mainly composed of coarse sand and fine particle. Its composition, property and phase vary with the type of the bauxite and the alumina production process, and will change over time. The chemical composition of the two kinds of red mud is

Table 2.1 The main chemical constituents of red mud (%) [2]

Chemical Constituent	Fe_2O_3	Al_2O_3	SiO_2	CaO	Na_2O	TiO_2
Bayer process	26.41	18.94	8.52	21.84	4.75	7.40
Sintering process	7.95	10.36	17.29	40.22	3.53	7.14

2.1.2 Uses of red mud

The comprehensive utilization of red mud can be divided into the following aspects.

First, recovery of Fe, Al, Na, and rare earth elements like Sc, Y, La, Ti, V [6–10] in red mud

Second, reuse of red mud as cement production and other construction materials like brick, glass and aerated concrete block

Third, utilization of red mud as road base material and filling material in mining and plastic

Fourth, application of red mud to absorb heavy metal ions like Cu^{2+} , Zn^{2+} , Ni^{2+} , Cd^{2+} , and non-metallic ions and molecules like NO_3 in the wastewater

Fifth, red mud can absorb heavy metal ions in the soil and SO_2 in the waste gas [1]

2.2 General Theory and Classification of Membranes

Membranes have gained an important place in chemical technology and are used in a broad range of applications. The key property that is exploited is the ability of a membrane to control the permeation rate of a chemical species through the membrane. In separation applications, the goal is to allow one component of a mixture to permeate the membrane freely, while hindering permeation of other components.

General terms and concepts of used in any kind of filtration process are enlisted below in brief.

Permeate: The part of feed stream, which can pass through the pores of the membrane.

Retentate: The part of feed stream, which is rejected by membrane on account of factors like high molecular weight compounds.

Rejection (R) %: The rejection % for any molecule, i is given by the equation

$$\text{Rejection (R) \%} = \frac{C_i - C_p}{C_i} \times 100 \quad (2.1)$$

Where C_p is concentration in the permeate while C_i is concentration of feed.

Flux: Flux may be defined as the total volumetric flow rate per area of membrane given by the equation

$$J = \frac{Q}{A} \quad (2.2)$$

Where K is permeability, ΔP_h is hydrostatic pressure difference, ΔP_i is osmotic pressure difference and l is the membrane thickness.

Molecular weight cut off: This term is particularly associated with polymeric membranes and generally expressed as MWCO. It refers to molecular weight (in Daltons) of species, which would be giving at least 90% rejection during process.

Concentration polarization: This is a phenomenon commonly encountered in most of membrane process which results in flux reduction drastically. When large colloids, macromolecules such as proteins are filtered, membrane largely rejects these molecules and forms a viscous and gelatinous layer on the surface of membrane. This adds to total resistance to flow in addition to those offered by boundary layer and membrane. Major impact of this problem is felt in ultra-filtration technique where flux reduces due to increased solute concentration on membrane surface resulting in higher osmotic pressure.

The principal types of membrane are described briefly below

2.2.1 Isotropic Membranes

Microporous Membranes

A microporous membrane is very similar in structure and function to a conventional filter. It has a rigid, highly voided structure with randomly distributed, interconnected pores. However, these pores differ from those in a conventional filter by being extremely small, on the order of 0.01 to 10 μm in diameter. All particles larger than the largest pores are completely rejected by the membrane.

Nonporous, Dense Membranes

Nonporous, dense membranes consist of a dense film through which permeates are transported by diffusion under the driving force of a pressure, concentration, or electrical potential gradient. The separation of various components of a mixture is related directly to their relative transport rate within the membrane, which is determined by their diffusivity and solubility in the membrane material.

Electrically Charged Membranes

Electrically charged membranes can be dense or microporous, but are most commonly very finely microporous, with the pore walls carrying fixed positively or negatively charged ions. A membrane with fixed positively charged ions is referred to as an anion-exchange membrane because it binds anions in the surrounding fluid. Similarly, a membrane containing fixed negatively charged ions is called a cation-exchange membrane. Separation with charged membranes is achieved mainly by exclusion of ions of the same charge as the fixed ions of the membrane structure, and to a much lesser extent by the pore size.

2.2.2 Anisotropic Membranes

The transport rate of a species through a membrane is inversely proportional to the membrane thickness. High transport rates are desirable in membrane separation processes for economic reasons; therefore, the membrane should be as thin as possible. Conventional film fabrication technology limits manufacture of mechanically strong, defect-free films to about 20 μm thickness.

2.2.3 Ceramic, Metal and Liquid Membranes

The membrane materials are organic polymers and, in fact, the vast majority of membranes used commercially are polymer-based. However, in recent years, interest in membranes formed from less conventional materials has increased. Ceramic membranes, a special class of microporous membranes, are being used in ultrafiltration and microfiltration applications for which solvent resistance and thermal stability are required. Dense metal membranes, particularly palladium membranes, are being considered for the separation of hydrogen from gas mixtures, and supported liquid films are being developed for carrier-facilitated transport processes.

2.2.3.1 Ceramic membranes

This kind of membranes refers mainly to those prepared with porous ceramics like alumina, silica, clay or substrates like titania and zirconia. These membranes find applications predominantly in the fields of solid-liquid separation and solid-gas separation. However, gas based separations also do exist with ceramic membranes. The structure of these membranes are unique with largest pore size are found at bottom as support and pore size decreases gradually towards the surface where the actual separation takes place. However these structures are highly amenable to modifications depending upon the selection of synthesis routes: from inner structures to top surface of membranes. The membrane is also available in different configurations like tubular, multi-channel monolith membrane etc. As indicated earlier, manufacturing method have an impact on membrane configuration and structural properties and some of methods are described.

Slip casting: This is the traditional method for membrane preparation where well mixed powder suspension are introduced, poured into a porous mould where solvent present is extracted into the pores of the mould via the capillary driving force. During this, the slip particles are consolidated on the surface of the mould to form a layer of particles which will not penetrate into mould as formation of this layer is ensured quite quickly. The pore size of the membrane is mainly dependent on the particle size of the powders used in the slip.

Tape Casting: This method is primarily used for synthesis of flat sheet ceramic membranes. Here, a powdered suspension is poured into a reservoir behind a casting knife. The carrier to be cast is set in motion and gap between the knife blade and carrier determines the thickness of the membrane formed. The important process variables are reservoir depth, speed of carrier and velocity of the powder suspension.

Pressing: This is most widely used method for the preparation of disc inorganic membranes. Here, the particle mix is subjected to high pressure force for consolidation into single mass and later on if required, sintered. Method finds application in screening new ionic and mixed conducting materials for development of oxygen or hydrogen permeable ceramic membranes.

Extrusion: This method is widely preferred for large scale manufacturing of membranes as well as bench scale. Here a stiff composite paste is compacted and shaped by forcing it

through a nozzle. The required condition is that, the precursor should exhibit plastic behaviour.

Sol-gel process: Sol-gel process for fabrication of membrane is opted when the pore size of the membrane has to be controlled at lowest levels. Two main routes for the preparation of membrane using this method:

Colloidal route- a metal salt is mixed with water to form a sol, which is coated on the membrane support to form a colloidal gel.

Polymer route- A metal-organic precursors are mixed with organic solvent to form a sol. It is then coated on the membrane support, where it forms a polymer gel.

Dip coating: Herein, a viscous suspension is coated on a suitable base and the critical factors are suspension viscosity, coating speed and time. Drying process starts simultaneously with the dip coating. To carry out multistep process, complete drying of initial coat is mandatory.

Chemical vapour deposition: The method takes help of chemical reactions to deposit a layer of the same or different compound. Reaction takes place mainly in gaseous medium surrounding the component. The experimental system consists of a system of a mixture of reactive and carrier gas, a heated reaction chamber, and a system for the disposal and treatment of exhaust gases. The products of a CVD system contain various hazardous components and particles. Thus, reaction side products are required to be treated before exhausting to the atmosphere.

2.3 Microfiltration of raw sugar cane juice

India is the world's largest producer of "plantation white" or "mill white" sugar by the double sulphitation process. A major challenge in this manufacturing scheme is to ensure that the clarification step consistently results in a juice of high clarity and low colour. However, variations in cane variety, changes in agro-climatic conditions and fluctuations in the manufacturing process lead to non-uniform juice characteristics. Further, the liming-sulphitation process employing conventional clarifier-settlers for removing the precipitated impurities is incapable of eliminating colloidal and dissolved macromolecular substances. For this reason, the clarified juice is typically slightly hazy and has a dark brownish yellow

colour. Thus the quality of plantation white sugar, characterized by a high colour and sulphite content, is noticeably inferior to refined sugar. Mineral membranes of molecular weight cut off (MWCO) up to 1 kDa (nearly in the NF range) were used in this study and it was found that even with the membrane of MWCO of 1 kDa, the maximum colour removal limited to 58.67% [4]. The MF process is found to be effective on turbidity and colour reduction of clarified sugarcane juice. Continued experiments showed optimum conditions of 70°C and 1.5 bars for the MF of clarified sugarcane juice. Experiments in 70°C and 1.5 bars reduced turbidity, viscosity and colour by 56.25%, 16.67% and 6.49%, respectively, and increased purity to about 0.87 units [5].

2.4 Ceramic MF/UF membranes for separation of crude-oil

A large volume of wastewater in the form of either oil-in water (o/w) or water-in-oil (w/o) emulsions is generated from various process industries such as metallurgical, transportation, food processing and petrochemical industries as well as petroleum refineries. The three broad categories in which industrial oily wastewater exist are free-floating oil, unstable oil/water emulsion and stable oil/water emulsion [10]. Free-floating oil or unstable oil/water emulsions can be readily removed by using conventional separation processes [11, 12]. However, for removing stable oil/water emulsion, those conventional processes are not found to be so effective. Cui et al. have reported the micro-filtration of oily wastewater using zeolite membrane with a pore size of 1.2µm and achieved 99% rejection for a feed concentration of 100 mg/L [13]. Nandi et al. have used a ceramic membrane for treatment of oily wastewater and investigated the effect of concentration oil-in-water and operating pressure on the rejection performance of the membrane [14] and Vasanth et al corroborated the findings. A maximum rejection of 85% is obtained through 1.3µm membrane for oil–water emulsion [15].

2.5 Characterization Techniques – An Overview

2.5.1 Scanning Electron Microscopy (SEM) & Energy Dispersive X-Ray Spectroscopy

Scanning Electron Microscopy (SEM), as the name suggest is an electron microscopy technique which provides the detailed information regarding sample's surface morphology, composition and other surface properties such as electrical conductivity. A high energy electron beam is directed towards the sample surface which interacts with the atoms that make up sample, and produce secondary electrons, back scattered electrons, characteristic X-

rays, light, specimen current and transmitted electrons which is detected with the help of special sensors to give high resolution images of sample surface morphology. When the high energy electron beam interacts with the electrons present in the sample, X-rays are emitted in this process, and these are used to identify the composition. It also measures the abundance of elements in the sample; characteristic feature of X-ray emitted depending up on the sample composition. The X-rays generated are mainly concentrated from a region 2 μm depth and hence EDX cannot be termed as purely a surface science technique.

The physical working of SEM involves, an electron beam being emitted from an electron gun, which is fitted with a tungsten filament cathode. Tungsten is used because of its highest melting point and low cost. The electron beam is condensed by one or two condenser lenses. When primary electron beam interacts with the sample, electron loses energy by repeated random scattering. The energy exchange between the electron beam and the sample, results in the reflection of high energy electrons, emission of secondary electrons and the emission of electromagnetic radiation, which can be detected, and so also the beam current absorbed by the specimen. This is used to create images of the specimen surface.

Sample Preparation: All the membrane samples for SEM analysis were dried for 10 hours prior to investigation to remove the trace amount of treatment solvent and moisture which may produce inferior quality images. The specific slot in specimen chamber was covered with carbon tape, on to which membrane was simply attached. For the surface morphology analysis of all membrane, samples were dried to remove moisture content and also ensured that sample size and thickness suited well to fit in the specimen chamber of equipment. Specimens were also coated with platinum by low vacuum sputter coating in order to increase the conductivity of the sample and to obtain superior image quality. The coated samples of membrane was simply placed over the specimen slot and locked into the chamber.

Scanning Electron Microscope in operation for this entire project purpose was SEM, JEOL JSM-6480 LV facility.

2.5.2 X-Ray Diffraction

X-ray diffraction technique is powerful characterization tool which provides information about the crystal structure, and physical properties of crystalline materials and thin films. In this technique, the scattered intensity of an X-ray beam generated upon hitting the sample is measured as a function of incident angle, scattered angle, polarization, and wavelength and as

pointed out by A. W Hull [52] in paper titled “A New Method of Chemical Analysis” that “Every substance produces a pattern, same substance produces always same pattern and in a mixture of substances each produces its pattern independently of the others”. Thus XRD patterns serves as a finger print of the each material.

In a typical analysis procedure of XRD machine, the sample is mounted on a goniometer and is gradually rotated with simultaneous bombardment of X-rays which after hitting the sample diffracts into different angles to generate two dimensional images at different positions. This data is integrated to obtain three dimensional data using mathematical method of Fourier transform, combined with the chemical data of the sample.

Although scattering of beams from the sample leads to destructive interference, there are specific directions in which they add up to give diffraction pattern governed by Bragg’s Law given by

$$(2.3)$$

Where θ is the incident angle, d is the spacing between the planes, n is any integer and λ is the wavelength of incident beam.

Sample Preparation: All the membrane sample for XRD analysis were dried for 10 hours prior to investigation to remove the trace amount of treatment solvent and moisture which may generate distorted patterns. For the analysis, membrane crystals were carefully placed in a sample slot to make powder bed and surface of powder was smoothened. Analysis of all the membrane samples was performed by placing the coated membrane surface upside into the sample slot in the equipment directly without powdering the sample. The synthesized samples were subjected to X-ray diffraction in 2θ angles ranging from 5° to 80° with a step size of 0.05 degrees and scanning rate 1° per minute.

X-ray diffraction machine utilized for this entire project purpose was XRD, Philips Analytical, PW-3040 equipped with the graphite monochromatized $\text{CuK}\alpha$ radiation ($\lambda=1.5406\text{\AA}$).

2.5.3 BET Surface Area Analysis

In 1938, Brunauer, Emmett and Teller (BET) introduced a new concept into the field of surface science which describes the multi-layer adsorption of gases over surfaces. This theory was later exploited to estimate the total surface area of material and is given by equation

$$\frac{v}{v_{mon}} = \frac{cx}{1-x} + \frac{x}{1-x} \quad (2.4)$$

Where x is relative pressure P/P_0 , v is the STP volume of adsorbate, v_{mon} is STP volume of the amount of adsorbate required to form a monolayer, c is the equilibrium constant.

A key assumptions used in development of BET equation is that the formation of multi adsorption layers unlike Langmuir theory (assumes monolayer adsorption of gases) and that successive heats of adsorption for all layers except the first are equal to the heats of condensation of the adsorbate. It also assumes that no multilayer formation occurs until monolayer adsorption of entire sample is completed. Another critical assumption is that there are no lateral interactions between adsorbed molecules. Hence, BET model describes the process of physisorption better than the Langmuir theory although it is generally still not a good model for adsorption on microporous materials. Micropores are not covered under this model as BET equation over estimates the surface area of microporous materials.

In a typical experiment, the sample to be analyzed is pre heated to remove maximum moisture. A known weight of dried sample is first known in the sample tube of known volume for a process called outgassing. Outgassing is performed in out gasser port of equipment prior to analysis in order to completely remove the moisture and gases already adsorbed in the micro and nano pores present sample. This outgassed sample is weighed and then employed for analysis in analysis port. Nitrogen gas is often used for analysis because of its well established molecular size, inert nature, availability in high purity and reasonable cost. The entire sample tube is immersed in a coolant bath of liquid nitrogen exposing it to lower temperature. At this point, a purge of nitrogen gas is introduced into the sample tube, which slowly gets adsorbed on the sample surface. The relative pressure of nitrogen is recorded against the volume of adsorbate and finally surface area of sample is estimated. All the operations are computer programmed using software supplied with equipment.

Sample preparation: Membrane samples for surface area analysis were dried initially at 100°C for 3 hours prior outgassing. The membrane sample in powder form was directly used for analysis. Well dried membrane was analyzed by taken a small chunk of sample of suitable size to fit into the tube and directly analyzed without powdering. The membrane samples were degassed at 150°C for 90 minutes.

The made of BET surface area analyzer employed during the studies of this project was Quantachrome - Autosorb-1.

2.5.4 Thermogravimetric Analysis

Thermal Gravimetric Analysis or Thermogravimetric Analysis (TGA) is an essential laboratory technique which is employed to predict the thermal stability of material by measuring the change of weight with respect to increase in temperature in controlled atmosphere. Based on the data obtained like weight loss, temperature and rate of temperature change, the information on absorbed moisture, proportion of organic and inorganic materials in sample, and solvent residue apart from degradation temperature is obtained after performing required transformation of the results for interpretation. Normally TGA can be conducted either in atmospheric environment or inert environment using nitrogen gas in pre-programmed gas flow rate. The heat flow change is also monitored to obtain differential scanning calorimetry data used for calculating enthalpy of reaction.

The experimental procedure involves placing a known weight of sample in a crucible kept on high precision sample which resides in a furnace. The temperature is gradually raised to our requirement and cooled down to room temperature and .the data acquisition system automatically plots the relation between temperature and weight loss which is finally smoothened to find the exact point of inflection. Derivative weight loss curve can identify the exact point of maximum weight loss and the temperature which indirectly provides degradation profile of the sample.

Sample preparation: membrane samples as obtained after synthesis were used after pre heating at 100°C to remove loosely bound moisture. Samples were subjected to maximum of 800°C at gas flow rate of 45 ml min⁻¹ and a consistent temperature ramp of 5°C min⁻¹.

Thermogravimetric analyzer employed for this project was from Shimadzu (DTG 60 H).

2.5.5 Mercury Intrusion Porosimetry

Mercury Intrusion Porosimetry is a powerful characterization technique for porous media including porous powders and porous membranes to obtain the data regarding pore size distribution and pore radius of macropores and mesopores, additionally information on the total porosity of sample. The working principle is based on Washburn equation which gives simple relationship between applied pressure and pore size given by

$$\text{—————} \quad (2.5)$$

Where r_p is the radius of pore which mercury intrudes, γ is the surface tension of the mercury and θ is the contact angle of mercury with the surface. Generally values of surface tension and contact angle are 480 mNm^{-1} and 140° .

Total pore volume is the total volume of mercury intruded at the highest pressure and mean pore diameter is calculated using the equation based on assumptions of cylindrical pores opened at ends.

$$\text{—————} \quad (2.6)$$

Volume pore size distribution is defined as the pore volume per unit pore diameter based on assumption of cylindrical pore shape and given by equation

$$\text{— — —} \quad (2.7)$$

Conventionally while modelling the diffusion characteristics through porous solids, its reported that effective diffusivity (D_{eff}) differs from the theoretical diffusivity or bulk diffusivity (D_b) related by a factor to structure of sample as follows:

$$\text{—————} \quad (2.8)$$

Where θ_c is the pore volume fraction and τ is the tortuosity factor. This effective tortuosity factor accounts for all the deviations from straight diffusion paths into a single dimensionless parameter value of which usually falls between about 1 and 7, with a value of 2 being associated with nonintersecting cylindrical pores.

A typical experimental procedure involves placing the sample in a special sample cup from which gas is evacuated and mercury is transferred to sample cell under vacuum. Then

pressure is applied to force mercury through the sample during which pressure and volume of mercury intruded is measured. As mercury is non-wetting liquid for most surfaces, it resists entering the voids and finally resulting in an intrusion-extrusion curve. Parameters required for describing pore structure of sample can be calculated from data obtained.

Sample preparation: Moisture free sample are prepared by drying the samples for 10 hours at 100°C. Moisture removal is very crucial since the presence of other liquids may interfere with the intrusion of mercury through the sample. Total weight and bulk density of sample is also determined prior the analysis. Pressure variation during intrusion was from 0.398 *psia* to 31841.545 *psia* and during extrusion it was 31538.537 *psia* to 21.464 *psia*.

Hg porosimeter employed during this project was from Quantachrome-Poremaster 32.

Chapter 3

EXPERIMENTAL WORKS

3.1 Introduction

Illustrative documentation on all the experiments performed during our study followed by various characterization steps followed to evaluate the membrane properties are clearly explained in this chapter.

3.2 Chemicals Utilized and Characterization

3.2.1 Chemicals

All the chemicals were obtained from commercial sources and utilized without any further purification unless specified. All the chemicals with their molecular formula and manufacturer are listed below:

Kaolin, [*Loba Chemie Labrotary Reagents Fine Chemical*]

Sodium carbonate [Na_2CO_3 , *Merck Specialities Private Limited, India*],

Sodium metasilicate [$\text{Na}_2\text{O}_3\text{Si}$, *Merck Specialities Private Limited, India*],

Boric acid [H_3BO_3 , *Merck Specialities Private Limited, India*]

Aluminium-tri-sec butoxide [$\text{Al}[\text{OCH}(\text{CH}_3)\text{C}_2\text{H}_5]_3$, *Fluka, Sigma Aldrich Chemie GmbH, Germany*]

3.2.2 Membrane characterization

Characterization was performed using SEM, Powder PXRD, FTIR, BET surface area analyzer and mercury porosimetry. The membrane morphologies were observed via scanning electron microscopy (SEM, JEOL JSM-6480 LV) equipped with an energy dispersive X-ray spectrometer and SEM to determine average pore size and pore size distribution Porosity. Prior to imaging, each sample was platinum coated in a specialized device to increase the conductivity for a better imaging. The synthesized samples were subjected to X-ray diffraction by a diffractometer (XRD, Philips Analytical, PW-3040) equipped with the graphite monochromatized $\text{CuK}\alpha$ radiation ($\lambda=1.5406\text{\AA}$) in 2θ angles ranging from 20° to 80° with a step size of 2 degree and scanning rate 1 minute. BET surface area analysis was performed by BET surface area analyzer (Autosorb-1, Quantachrome). The relative pressure

in BET surface area calculation was between 0.05-0.35. Thermal stability of samples was carried out in detail in a TGA apparatus, Shimadzu (DTG 60 H). Using mercury intrusion porosimetry we can find Pore size distribution and pore radius of macropores and mesopores, additionally information on the total porosity of sample. Water permeation experiments were carried out to evaluate the average pore size and permeability. Chemical stability of the membranes was checked by comparing the porosity, pore size.

3.3 Fabrication of membrane

Concept of synthesis of membranes using the red mud and composition of red mud was described by Ping Wang et al. [2]. Fabrication procedure followed by Jana et al. [15]. We collected red mud from aluminium industry. We followed a method known as paste casting for fabricating the support and hence the final membrane. The details are given below:

The red mud collected was made free from all the impurities such roots, plastic pieces and leaves, followed by drying in sunlight for 7 days for complete moisture removal. Dry red mud was fed into a ball mill for 3 hours to reduce particle size of soil so that paste made for membrane support preparation yield good viscous properties. The resultant fine powder was sieved with BSS 36 mesh screen. The composition of membranes is given below in Table.3.1 and Table.3.2 for membrane A and membrane B respectively as per Jana et al [17-18].

Table 3.1: Composition of membrane A (without kaolin)

Materials	Wet Basis	Dry Basis
Clay (%)	58.26	85.81
Sodium Carbonate (%)	5.01	7.38
Sodium Meta Silicate (%)	2.40	3.54
Boric Acid (%)	2.20	3.252
Water (%)	32.10	0

The membranes were prepared by paste casting techniques [15]. The materials were mixed with distilled water and the paste was casted over an aluminium foil in the shape of circular discs of 52mm diameter and 6 mm thickness. After partial drying in room temperature for 24 h, the disc was removed carefully and heated at 100°C for 12 h. The temperature was then raised to the desired sintering temperature (800°C and 900°C respectively) and heated for 6 h. After this isothermal treatment, the temperature of the muffle furnace was cooled gradually to room temperature. Membranes were finally polished with silicon carbide abrasive paper (C-

180), to give a good aesthetic look. Ample care was taken while sintering and cooling down so as to avoid crack formation on membrane support surface. Each additive has got their own properties influencing the membrane properties. The components sodium metasilicate increases mechanical strength by creating silicate bonds, sodium carbonate improves dispersion properties, thereby creating homogeneity and boric acid also increases mechanical strength of support by creating metaborates during sintering. Two types of membranes were fabricated in this process and named *membrane A* and *membrane B* throughout the literature.

Table 3.2: Composition of membrane B (with kaolin)

Materials	Wet Basis	Dry Basis
Clay (%)	46.66	56
Kaolin (%)	13.33	16
Sodium Carbonate (%)	3.33	4
Sodium Meta Silicate (%)	1.66	2
Boric Acid (%)	1.66	2
Water (%)	16.66	0

3.4 Permeation and filtration experiments

Any kind of membrane fabrication and related studies gains importance only if an experiment elaborating its permeation characteristics and separation efficiency for a particular feed condition is performed.

3.4.1 Design of Filtration set up

The hydraulic permeability and filtration experiments for clay support and MOF membrane respectively were achieved through the experimental set up as shown in Figure 3.1

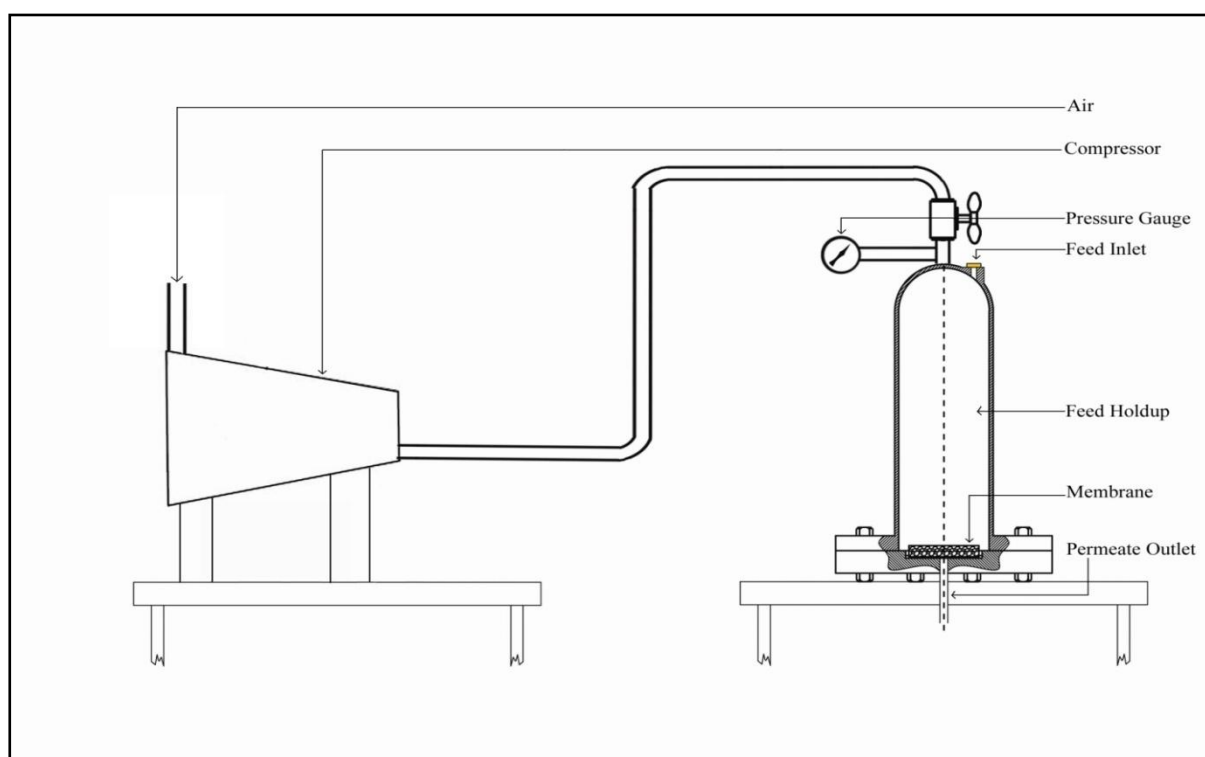


Figure.3. 1Schematic Diagram of Experimental set up for permeation and separation studies

As clearly shown in Figure 3.1, experimental set up may be partitioned into two main parts viz. membrane module and compressor section, each described below.

- *Membrane Module:* The home made membrane module made of stainless steel consists of two parts; feed hold up section and grooved membrane holding plate, with extended flanges bolted tightly together. Feed hold up section is a hollow cylindrical portion capable of holding 300 ml of feed per batch. Top of cylinder consists of inlet

port for introduction of feed and valve connecting the line to compressor for passage of compressed air. A pressure gauge is also fitted in order to measure the pressure at the time of filtration. Membrane holding plate is a circular disk, designed to hold membrane tightly during the process. It consists of concentric circular grooves (shown below), with a provision to incorporate an 'O' ring, which help to arrest the possible leakage upon pressurizing the system. The flanges holding both parts are tightened with 'nut and bolt' arrangement in order to leak proof the system

- *Compressor Section:* Compressor as shown in Figure 3.1 supplies compressed air to the membrane module, hence pressurizing the feed to the required level. The pressure gauge monitors the system pressure and the system pressure is adjusted using the valve.

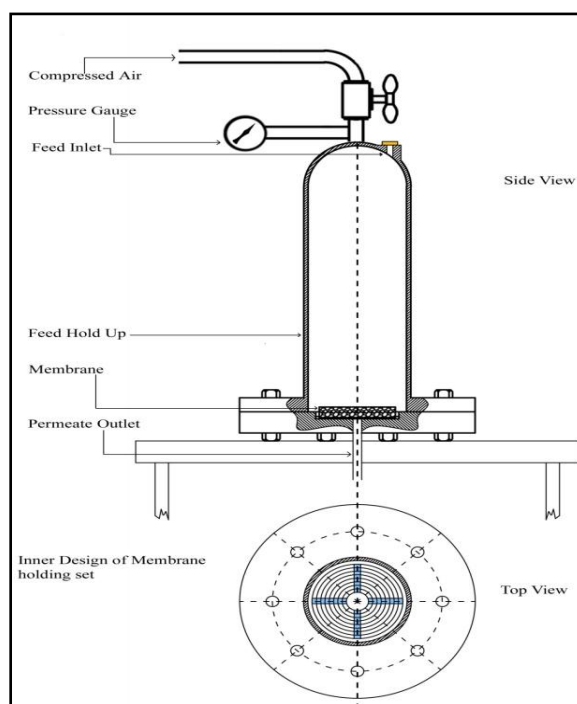


Figure.3.2 Side view and Top View of Membrane Module

3.4.2 Hydraulic Permeability studies

Hydraulic Permeability or Conductivity represents the ease with which water permeates through the porous media particularly through rocks or soil. It largely depends on the intrinsic permeability of material and degree of saturation of media. The hydraulic studies of clay supports (both normal and HCl treated supports) were carried out using the standard membrane module shown in Figure III.1. Distilled water was used for all the experiments.

Hydraulic permeability (L_h) and average pore radius (r_l) of membrane were determined using equation suggested by Almandoza et al. [63]

$$\text{---} \quad (3.1)$$

Where, J is the liquid flux ($\text{m}^2 \text{m}^{-2} \text{s}^{-1}$), ΔP is the transmembrane pressure (in kPa), μ is the viscosity of water and l is the pore length (assumed as membrane thickness). Considering porosity of sample as $\epsilon = n\pi r^2$, Equation (3.1) changes to

$$\text{---} \quad (3.2)$$

Porosity was figured out using the principle of Archimedes' [64] given by equation

$$\text{---} \quad (3.3)$$

Where, m_D is the dry support mass, m_w is the mass of the support with pores filled with water (pores are filled with water under vacuum), m_A is the mass of the water saturated support measured in water (A refers to Archimedes'), and P is the porosity.

All the experiments were performed at room temperature and pressure maintained at 300 kPa. Membrane support was fixed tightly using commercially available epoxy resin 'M-Seal' to the grooved membrane plate. A very high flux was observed at the initial stages but reduced gradually to steady state value with time due to compaction of membrane. Permeate volume with respect to time was noted down to study flux variation and the steady state flux was used to calculate the hydraulic permeability and estimate pore radius. The rejection was calculated using the Equation 3.4 given below.

$$\text{---} \quad (3.4)$$

3.4.3 Separation of crude oil from crude oil –water emulsion

3.4.3.1 Experimental protocol for feed preparation & estimation of crude-oil water emulsion

Feed preparation

Crude oil was obtained from the Indian Oil Corporation Limited refinery located at Rajahmundry, Andhra Pradesh, India. For preparation of homogenous phase of crude oil with water, 10 ml crude oil was mixed with 90 ml of water and mixed well with stirrer at high rpm for 3 hours. Then the resulting solution was sonicated in bath sonicator for 10 minutes to further destruct the oil layer and then again mixed well enough using stirrer for 1 hour. Upon sonication, oil breaks into fine droplets in aqueous medium forming stable emulsion. Emulsion is characterized by milky white solution and a very fine layer of oil slick on the top.

This solution was used for separation studies and prior to the experiment, a sample of initial mixture was used for spectrophotometer analysis of crude. Enough care was taken so as to discard the oil slick in sampling as we require only the concentration of oil in milky white system.

Analytical procedure for estimation of crude oil

Method for quantitative estimation of crude oil was adopted similar to the method as described elsewhere [15-16]. Initially standard calibration curve was obtained using pure crude oil with n-hexane as solvent as crude oil completely dissolves in n-hexane. The standardization of crude oil concentration with respect to optical density is elucidated below.

- A crude oil working solution was prepared by adding 200 μ l oil in 10 ml hexane system. An adequate amount of working standard was pipetted out to obtain variation of concentration of oil in each test tube.
- A set of 6 test tubes were taken and 0, 10, 20, 30, 40 and 50 μ l of working standard diluted to 10 ml system with n-hexane were used.
- Solution was mixed well and the absorbance of each solution was read in wave length range of 200-350 nm.

Maximum absorbance was obtained at 223 nm and optical density at this wave length was used to plot standard curve. The concentration of crude oil was determined by standard curve for all the experiments further.

Quantitative estimation of crude oil in permeate

Even though a stable emulsion is obtained, the two phase mixture forming translucent solution is not suitable for spectrophotometer analysis. Hence we devise a method to calculation of crude oil concentration based on mass transfer of oil between permeate and n-hexane and described as follows:

- Two milliliters of permeate was collected and mixed with equal volume of n-hexane to form a two phase solution.
- 100 μ l of hexane from two phase mixture is taken and diluted to 5 ml system using n-hexane as solvent.
- Optical density of resulting sample was measured using spectrophotometer at 223 nm. (Wave length of maximum absorbance)

Calculation of concentration of solution is completed using the standard calibration data and corresponding rejection % has been calculated. Even though calculation of concentration is mainly dependent on the mass transfer of crude oil between the water and hexane, since all the procedures are performed in standard conditions, we can obtain a relative value of concentration of crude in all samples. But rejection percentages can be considered as absolute values and they are calculated with respect to time.

3.4.3.2 Filtration experiments

Separation experiment was performed using the permeation set up previously described (*See Section 3.4.1*) using dead end filtration technique. Feed solution was carefully poured and whole module was perfectly sealed using Teflon tape to avoid leakage of pressure and liquid. For the experiments, liquid feed was pressurized using compressed air from compressor. Pressure was maintained at 3 kg cm⁻² throughout the process. To assess the quality of separation, quantitative estimation of crude oil in permeates was checked at regular intervals taking spectrophotometer reading and corresponding time was noted down. Sampling was performed at regular time interval in order to ascertain if there was any variations of quality of permeate obtained with respect to time. Permeate volume was also noted to find the variation of flux with respect to time since possibility of choking of membrane due to oil film formation couldn't be ruled out. It should be noted that the experiments were performed in batch process with no recycle.

3.4.3.3 Membrane recoverability

Attempts to recover the support and membrane were pursued by back washing and permeating first with n-hexane followed by acetone and water. During the initial step, n-hexane was used which dissolves all the crude trapped on surface and pores. Acetone being soluble in n-hexane removes all n-hexane from support surface and acetone is finally removed by washing with water.

Performance of the recovered membranes was checked by performing hydraulic permeability studies once again to determine the flux.

3.4.4 Clarifying sugar cane juice

3.4.4.1 Experimental protocol for feed preparation and estimation of sugar cane juice

Feed preparation

Raw sugar cane juice collected from locally available market. Store it in freeze at round -10°C. Adjust it to 16.32°Brix and heat it around 65°C for 30 min. Keep the heated sugar cane juice in a undisturbed place for around 2hr for solid particles agglomerate and settled down. Filter the juice with what man's filter paper.

Analysis of sugar cane juice

The juice brix (total dissolved solids - %) and pol (apparent sucrose content - %) were measured using a refracto meter and a Laurent's half-shade polarimeter, respectively. The juice purity was calculated from the brix and pol, the pH was determined by a Digimed DM-20 pH-meter.

The juice colour estimation was realized in accordance with ICUMSA (International Commission for Uniform Methods of Sugar Analysis) method. The juice samples were diluted to 16.32°Brix, filtered using a whatman filter paper, The juice colour (in ICUMSA unit - IU) was estimated as the absorbance index, measured at 900nm with a UV-spectrophotometer, and for turbidity absorbance unit measure at 420nm. And calculate purity, purity rise, pol percentage, colour using the following relations.

Where A_s is absorbance unit at 560nm for color and for turbidity it is 900nm of UV-spectroscopy, b is base length, RDS is refractory dissolved solid, and ρ is density of sugar cane juice at room temperature.

3.4.4.2 Filtration experiment

Separation experiment was performed using the permeation set up previously described (*See Section 3.4.1*) using dead end filtration technique. Feed solution was carefully poured and whole module was perfectly sealed using Teflon tape to avoid leakage of pressure and liquid. For the experiments, liquid feed was pressurized using compressed air from compressor. Pressure was maintained at 3 kg cm^{-2} throughout the process. To assess the quality of separation, quantitative estimation of sugar cane juice in permeate was checked at regular intervals taking spectrophotometer, refractometer, polarimeter reading and corresponding time was noted down. Sampling was performed at regular time interval in order to ascertain if there was any variations of quality of permeate obtained with respect to time. Permeate volume was also noted to find the variation of flux with respect to time. It should be noted that the experiments were performed in batch process with no recycle.

3.4.4.3 Membrane recoverability

Attempts to recover the support and membrane were pursued by back washing and rinsing with hot de-ionized water at 60°C for 30 min and clean with 2% of HNO_3 followed by 2% NaOH . Performance of the recovered membranes was checked by performing hydraulic permeability studies once again to determine the flux.

RESULTS AND DISCUSSIONS

This section elaborates various findings that we came across while carrying out experiments. All the observations are systematically noted down in the following paragraphs and carefully compared with the available literature.

4.1 Powder X-ray diffraction analysis

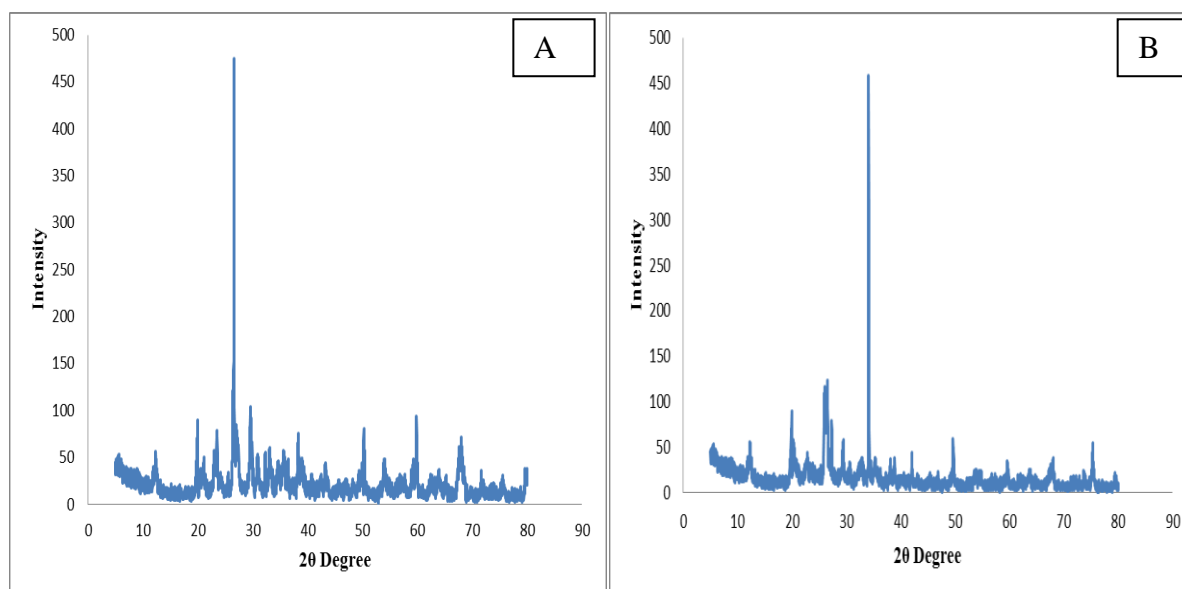


Figure 4.1 XRD analysis of Membrane A sintered at 800°C (A) and sintered at 900°C (B)

From XRD analysis (Figure 4.1 and 4.2), the compositions of membrane A and membrane B sintered at 800°C and 900°C are shown.

The major constituents of red mud is from literature, silica in the form of silicon dioxide (SiO_2), aluminium as aluminium oxide (Al_2O_3) and sodium as sodium oxide (Na_2O).but after sintering the membranes contents mullite , kaolinite . illite , quartz , nephiline these spectrum obtained from X-ray diffraction analysis of sample shown above figure. The XRD spectrum is matched with the JCPDs data base file (PDF-01-089-6538) which indicates the above materials.

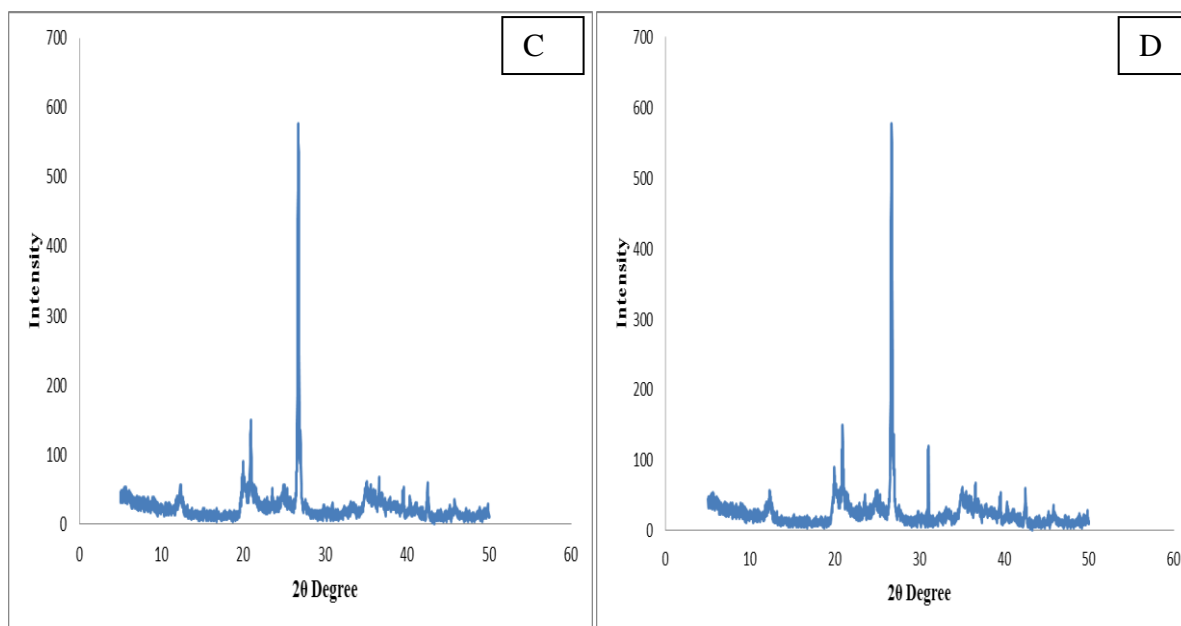


Figure 4.2 XRD analysis of Membrane B sintered at 800°C (C) and sintered 900°C (D)

In membrane A, peaks corresponding to illite, kaolinite and quartz and for membrane B, peaks corresponding to kaolinite, quartz and inyoite are observed and corroborated well with the literature data. In the sintered samples, no specific peaks for kaolinite were found due to its transformation to metakaolinite. For membrane A, peaks corresponding to quartz, mullite and nephiline are detected whereas in case of membrane B, peaks for quartz and mullite are seen. In Membrane B, there is an absence of inyoite after sintering. A critical observation of the peaks reveals that there is significant phase transformation occurring at higher temperature. This signifies that the membrane skeletal structure constitutes mainly metakaolinite, quartz and nephiline.

4.2 Scanning Electron Microscope (SEM) analysis

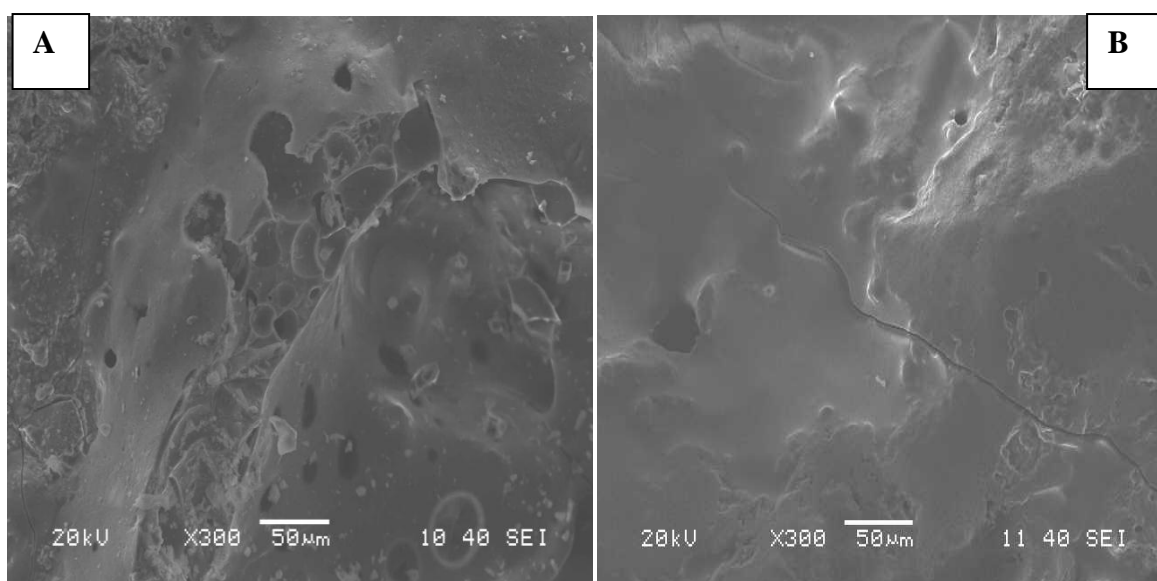


Figure 4.3 SEM images of **membrane A** (A) at 800°C and (B) at 900°C

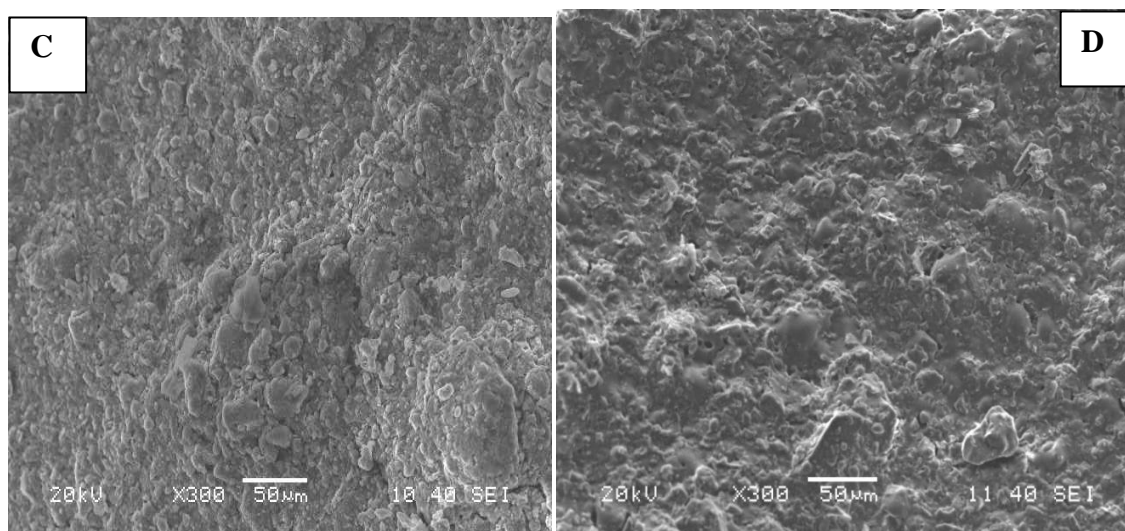


Figure 4.4 SEM images of **membrane B**, (C) at 800°C and (D) at 900°C

SEM pictures for the two different membranes of membrane A and Membrane B, sintered at two different temperatures considered in this work. All the membranes are shown in fig 4.3 and fig 4.4. All the membranes showed a surface with rough morphological structure. The ceramic substrates sintered at lower temperature shows highly porous structure and the structure of the membrane became dense. The membrane A detects the small cracks

on the membrane surface and sintered at 900°C (membrane A and membrane B) are more consolidated due to the fact that for sintering temperature over 850°C the particles agglomerate together creating more dense ceramic body. As a result the porosity of the membrane decreases with increase in sintering temperature (25-15%). A superficial observation of the SEM indicates that the membrane B did not have any pinholes cracks and the maximum observable pore size for the membrane A is about 10µm and for membrane B is 6µm.

4.3 Mercury porosimetry analysis of membrane

Clay support prepared by paste casting method were characterized using Hg porosimetry and support features like average pore size, pore size distribution, permeability and pore tortuosity were determined. Mercury intrusion curve with Pore size diameter vs. Cumulative pore volume from the intrusion Hg through the sample and is shown in Figure

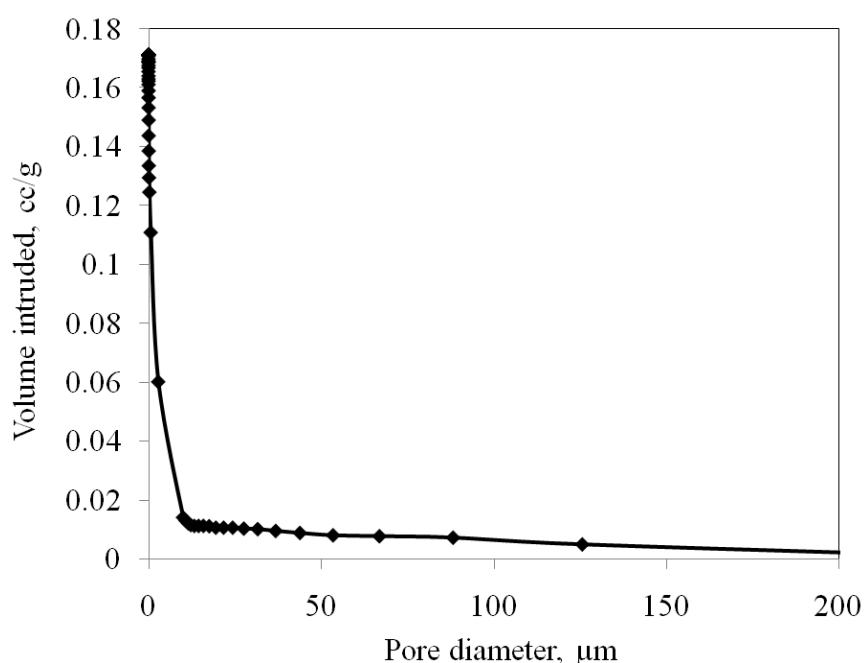


Figure 4.5 Multimodal pore size distribution of membrane A

The first step upward near 7 µm range may be attributed to macro pores present in the membrane sample. These are the pore mainly present in inter particle region which is resulted from the removal of CO₂ gas from the support upon decomposition of Na₂CO₃. Moreover as

the support is not subjected to any compression to high pressure while paste casting, this results in macro pore size range beyond 10 μm in synthesized support. The second and third step in the pattern near 0.07 μm and further near 0.01 μm is due to internal pore structure and properties of the mixture constituents.

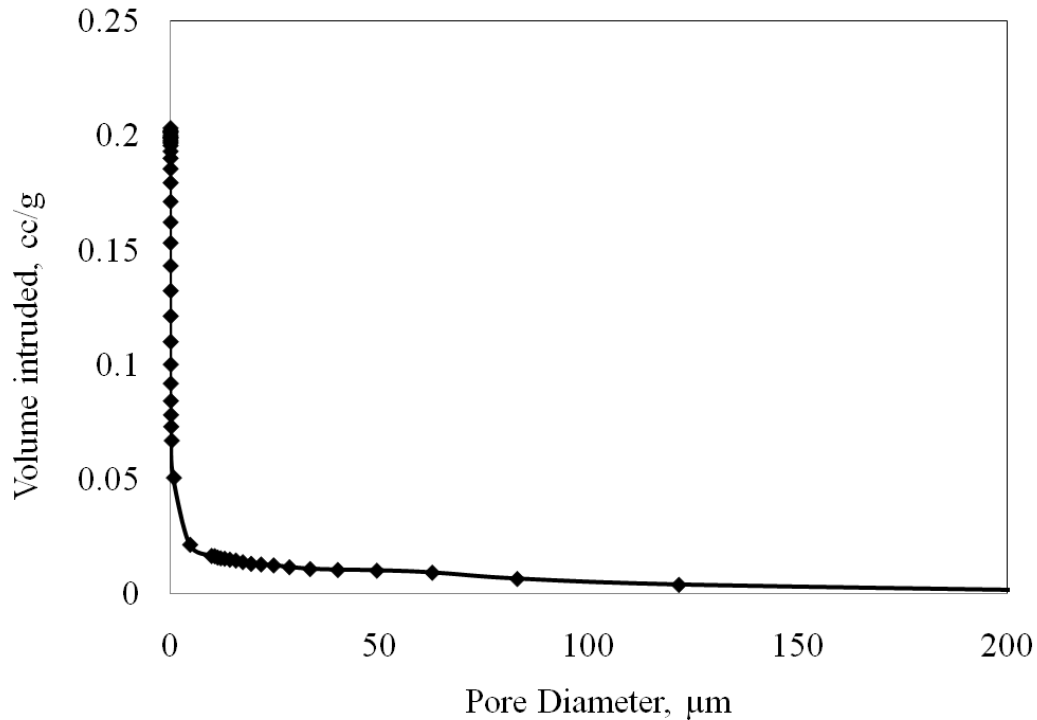


Figure 4.6 Multimodal pore size distribution of membrane B

The sample of clay support showed mean pore volume of 9.98×10^{-2} and $6.842 \times 10^{-2} \text{ cc g}^{-1}$ and a mean pore diameter of 17.2 and 2.27 μm of membrane A and B respectively.

Pore tortuosity of the porous media can also be obtained directly which can be used to predict pore shape and permeability. Conventionally while modeling the diffusion characteristics through the porous solids, it is reported that effective diffusivity (D_{eff}) deviates from the theoretical diffusivity (D_b) by a factor given by the following equation

$$\text{—} \quad (4.1)$$

Where θ_c is the pore volume fraction and τ is the tortuosity factor

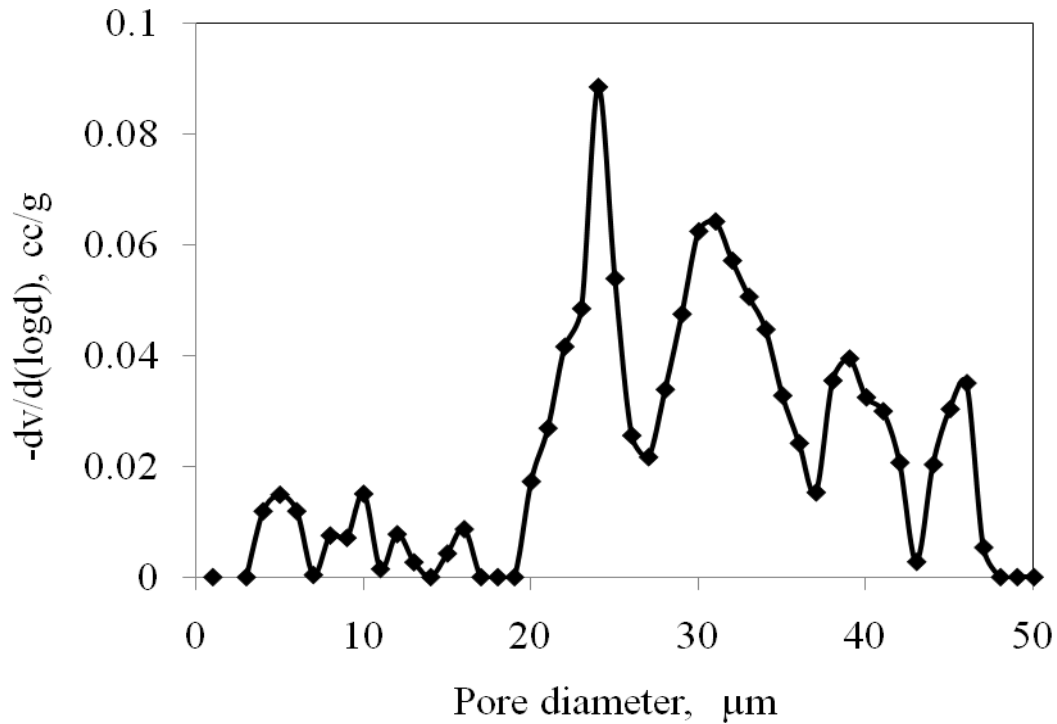


Figure 4.7 Pore size distribution of membrane A

This effective tortuosity factor accounts for all the deviation from the idealized straight diffusion paths into a single dimensionless parameter, value of which ranges from 1 to 7, with value approximating 2 signifies cylindrical pore shape. The tortuosity value for clay support is calculated to be 2.13 and 2.02 of membrane A and B respectively, which is a reasonable assumption for presence of cylindrical pores suitable for permeation of liquid smoothly.

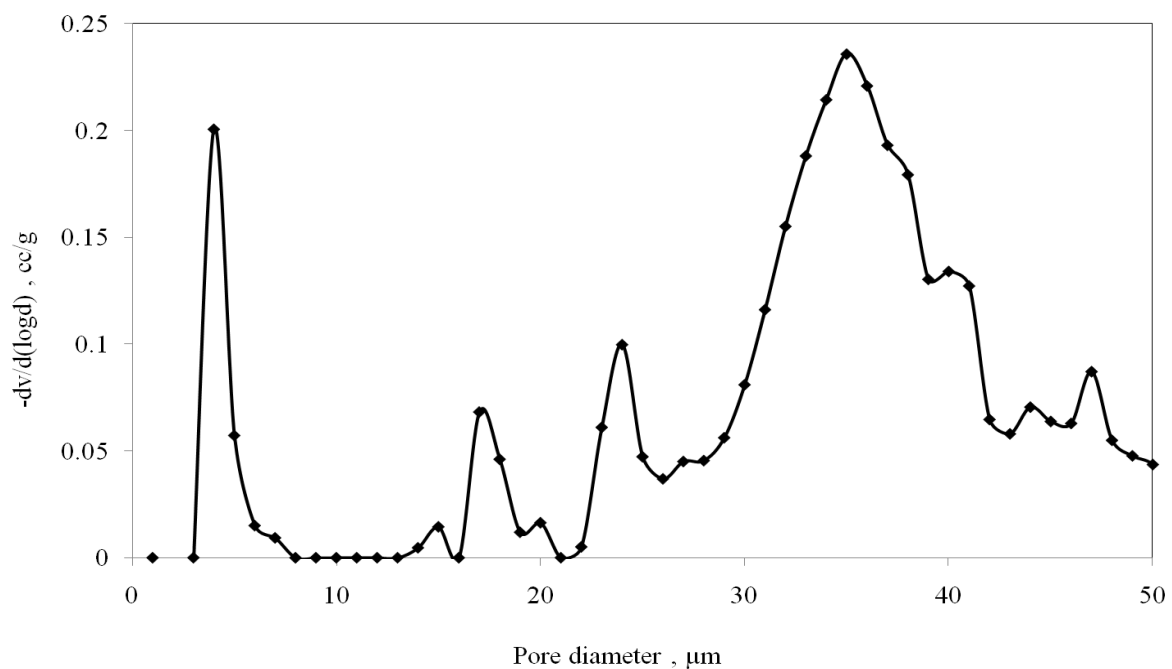


Figure 4.8 Pore size distribution of membrane B

Estimation of permeability “K” can be done using the data obtained Hg intrusion curves. The requisite for estimation of K is based on assumption of a model on pore structure of sample. This model is generally considered as a bundle of capillaries which is regarded as frame of reference. For samples studied, the tortuosity value is approximately 2.0; and the model for the flow of fluids across straight cylindrical channels in bed of powder by combining Darcy’s law and Poiseuille’s laws is applied. The permeability values, neglecting tortuosity effects, $K_n = 1.1270\text{E-}03 \text{ nm}^2$ and accounting for tortuosity effects, $K_t = 1.1103\text{E-}03 \text{ nm}^2$.

Total porosity of membrane A sintered at 800°C is estimated to be approximately 18.85 %, intra particle porosity of 13.20% and inter particle porosity: 5.64 %.

Total porosity of membrane B sintered at 800°C is estimated to be approximately 37.71 %, intra particle porosity of 21.59% and inter particle porosity: 16.11 %.

4.4 BET Surface area analyser

Using the BET surface area analysis we can find the surface area of the material. BET surface analysis is regarded to be an important characterization technique for ceramic membrane. The BET isotherm obtained for 'Red mud' is shown in figure below.

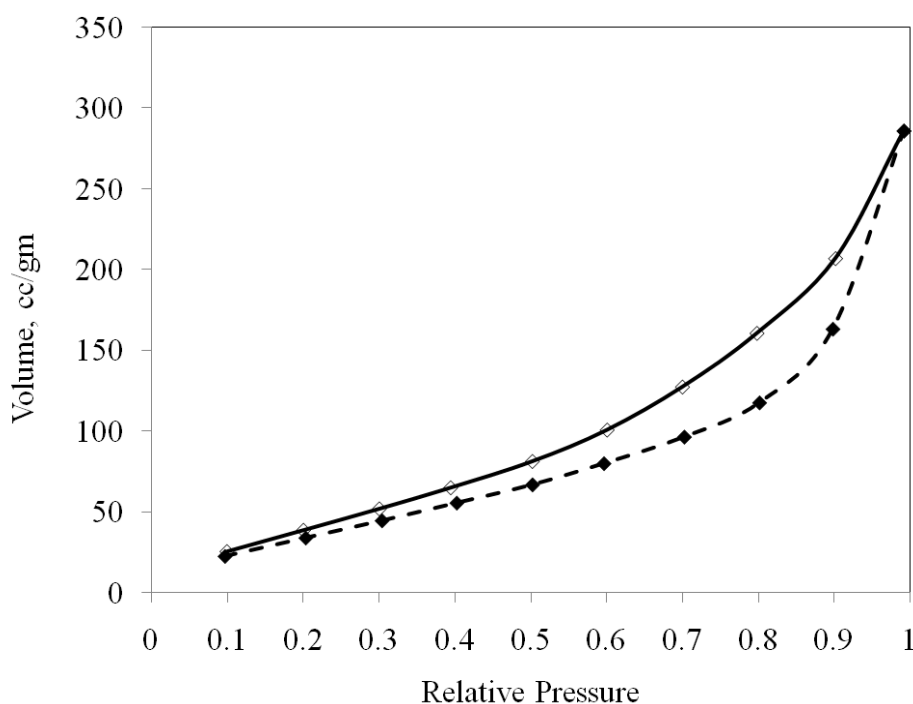


Figure 4.9 BET Isotherm of Red Mud

BET isotherm studies were performed in the relative pressure range of 0.1 to 1.0. The figure shows the complete adsorption and desorption curves. From the adsorption-desorption isotherm pattern, it can be interpreted that no hysteresis was observed and hence we can safely assume pores of the membrane are cylindrical in shape. For BET surface area, isotherm is valid within a relative pressure between 0.1-1.0, giving total surface area of Red mud is $34 \text{ m}^2 \text{ g}^{-1}$.

4.5 Thermo gravimetric (TGA) analysis

Thermal Gravimetric Analysis or Thermo gravimetric Analysis (TGA) is an analytic method. This measures the change of weight with respect to increase in temperature in a controlled. Atmosphere thus to predict the thermal stability of the material tested. The primary parameters measured during analysis include weight, temperature and rate of temperature change. These data are plotted after required transformation before the results are interpreted. Based on the interpretation, this analysis gives information on absorbed moisture, proportion of organic and inorganic materials in sample, and solvent residue apart from degradation temperature. A typical experiment involves placing a known weight of sample in the crucible and gradually raising the temperature which can be programmed according to our requirement.

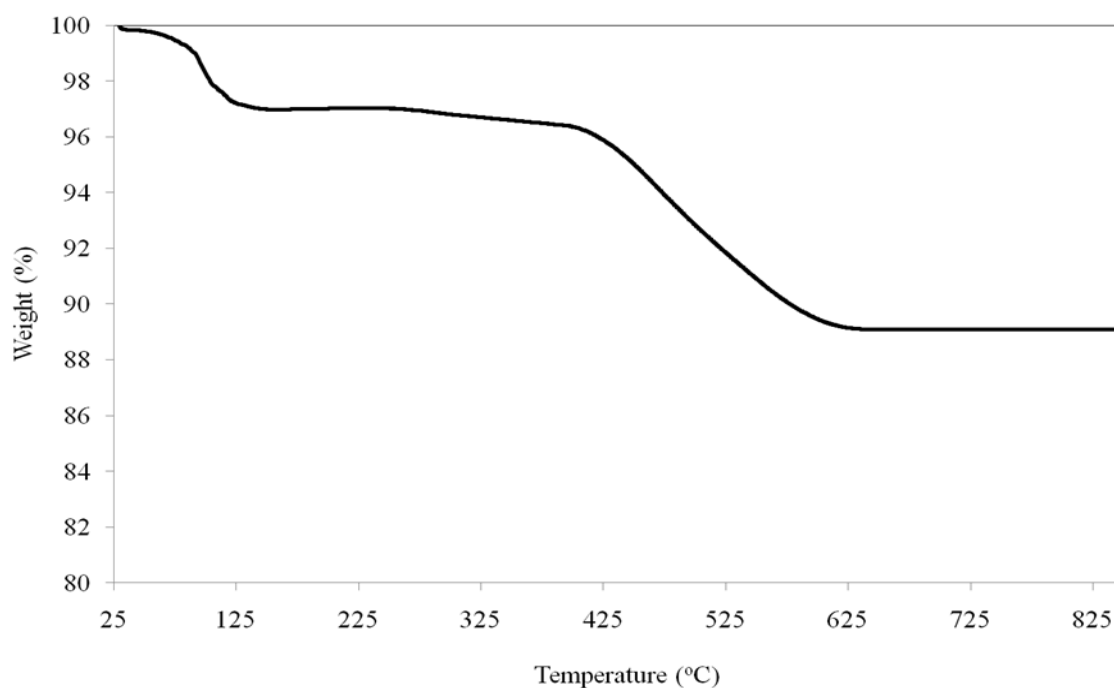


Figure 4.10 TGA Pattern of membrane before sintering

During the first phase of heating the mass loss of membrane up to 90 °C was 0.23% and upto 150 °C the mass loss of membrane had shown a mass loss of 2%. These mass losses can be attributed to the loss of loosely bound water molecules. The higher mass loss was due to the presence of some hygroscopic materials (like sodium metasilicate, boric acid). At temperatures up to 750 °C, it was observed that the higher mass loss of membrane is occurred

between 300 °C to 600 °C. This phenomenon may be attributed to the fact that the boiling point of boric acid as a component in membrane is around 300 °C. After 750°C for the compositions, mass change was marginal. Thus, the minimum sintering temperature for the membranes should be above 750 °C.

4.6 Permeation experiment

The inorganic membranes are subjected to liquid permeation test using deionized water in batch mode operation. The hydraulic permeability, average pore diameter and porosity of the membrane are determined experimentally. Transmembrane pressure drop for water permeation test is maintained at 0-250kpa (microfiltration range). Before using each fresh membrane, membrane compaction has been conducted using deionized water at a transmembrane pressure 300kpa. During these experiments, the membrane flux was observed to be high initially and reduced to a steady state. At beginning flux of $1.96 \times 10^{-4} \text{ m}^3 \text{ m}^{-2} \text{ s}^{-1}$ which reaches to steady state value of $4.23 \times 10^{-5} \text{ m}^3 \text{ m}^{-2} \text{ s}^{-1}$ shown in fig (4.11). These data was taken by measuring the permeate of 250ml volume. The hydraulic permeability and average pore radius of the membrane can be estimated according to the Eq (1). The average pore radius of the membrane is evaluated by assuming presence of cylindrical pores in the membrane matrix using the Eq (2). The porosity of the membrane is determined by pycnometric method using water as wetting liquid. The porosity of membrane A is decrease from 18.85% to 16.52% when sintering temperature is 800°C and 900°C respectively and for membrane B 19.25% to 17.36 .this is due to the fact that increase in sintering temperature densification of the porous structure occur and thereby allow for an decrease in the membrane porosity.

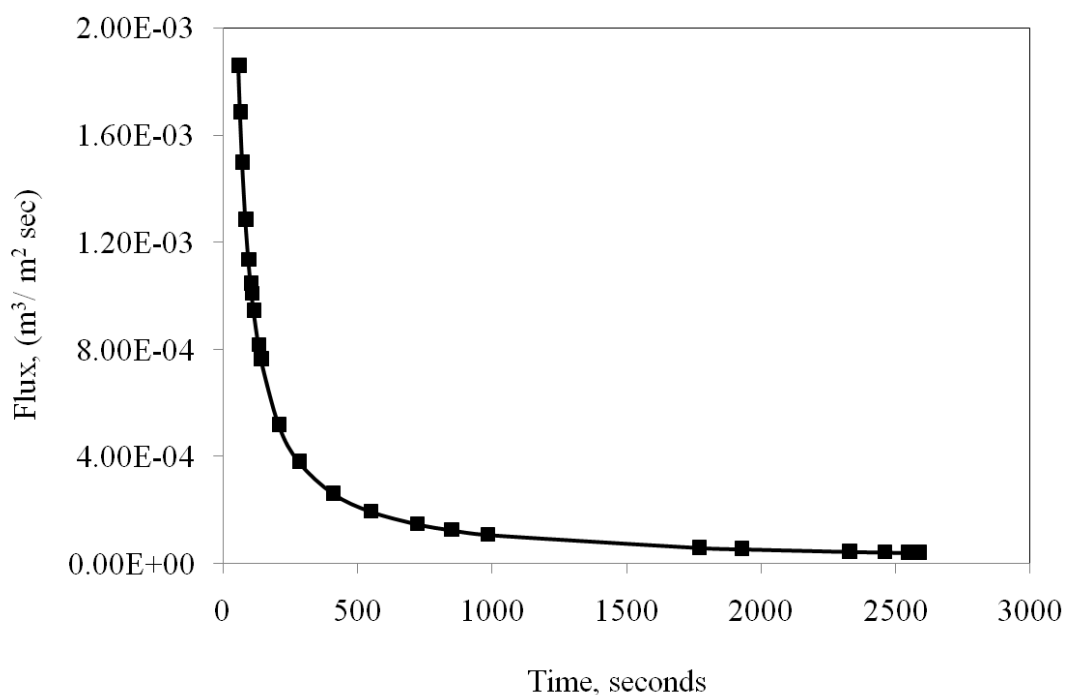


Figure.4.11 permeate flux (deionised water)

4.7 Separation experiment

Two Separation experiment where performed.

(1) Microfiltration of sugarcane juice and (2) separation of crude oil from crude oil-water emulsion with two different membranes *viz.* *membrane A* (**without kaolin**) and *membrane B* (**with kaolin**)

4.7.1 Microfiltration of sugar cane juice

Feed preparation: The sugarcane juice was collected from locally available market, and freeze-stored at -10°C . The reading of refractometer is 33.6°Brix and we have to adjust it 16.3°Brix with adding distilled water. And heat the juice at 65°C for 30 min solid particle agglomerate together and settled down, for this process keep the solution in undisturbed place for 2hr, and passed through what man filter paper.

The typical quality parameters of feed and permeate streams of different TMP is given in [Table 3](#). It can be seen from the sample the average values of turbidity and colour of the feed

stream generally tend to increase with time due to concentration but the °Brix and pol of the feed stream did not change much.

Table.4.1 Comparison of juice properties (permeate)

Property	Feed	Permeate of membrane A	Permeate of membrane B
pH	5.8	5.78	5.76
°Brix	16.3	15.6	15.56
Pol (%)	14.2	13.89	13.82
Turbidity (absorbance units)	0.34	0.05	0.09
Color (absorbance units)	0.76	0.57	0.65

Separation experiment was performed using the permeation set up previously described using dead end filtration technique. Feed solution was carefully poured and whole module was perfectly sealed using Teflon tape to avoid leakage of pressure and liquid. For the experiments, liquid feed was pressurized using compressed air from compressor. Two different membranes of A and B with Trans-membrane Pressure was maintained 300 kPa throughout the process. To assess the quality of separation, quantitative estimation of sugar cane juice in permeate was checked at regular intervals taking spectrophotometer, Refractometer, Polarimeter, and pH meter reading and corresponding time was noted down. Sampling was performed at regular time interval in order to ascertain if there was any variations of quality of permeate obtained with respect to time. Permeate volume was also noted to find the variation of flux with respect to time since possibility of fouling of membrane due to solid layer formation couldn't be ruled out. It should be noted that the experiments were performed in batch process with no recycle.

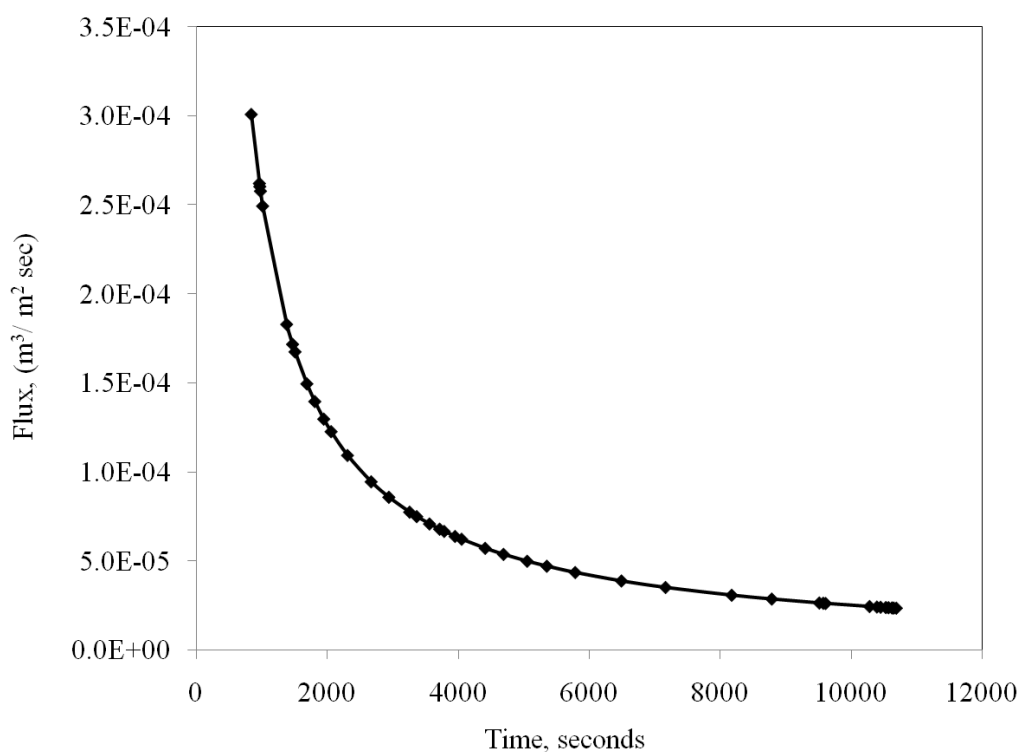


Figure.4.12 Permeate flux of sugar cane juice at 300 kPa of membrane A

The study of the microfiltration of sugar cane juice with two different membrane on colour & turbidity reduction, and permeate flux, we conducted two experiments of two different membrane of TMP 300 kPa using 16.2 °Brix solutions and a membrane (A & B) sintered at 800°C. The temperature of the sugar solution is at room temperature. The reduction in colour, turbidity, with different flux and pressure are shown in Table 4 and Table 5. The average flux of membrane A and membrane B obtained at 300 kPa is $9.0584 \times 10^{-5} \text{ m}^3 \text{m}^{-2} \text{s}^{-1}$ (327.018 litre/m² hr) and $1.625 \times 10^{-5} \text{ m}^3 \text{m}^{-2} \text{s}^{-1}$ (59.566 litre/m² hr) respectively.

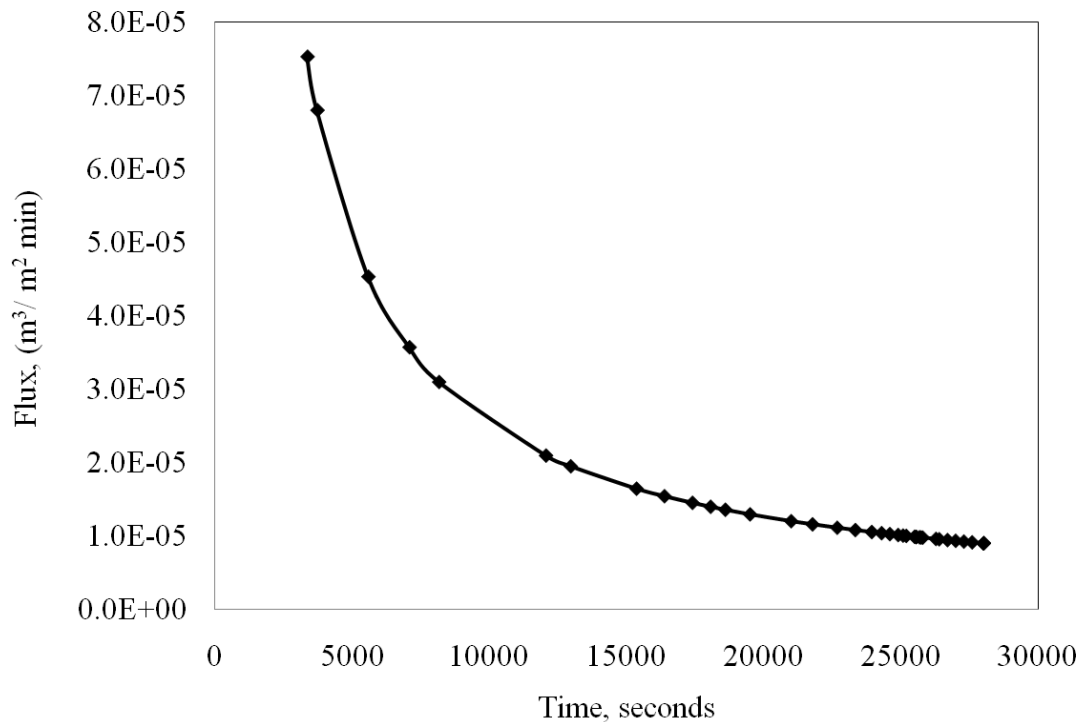


Figure 4.13 Permeate flux of sugar cane juice at 300KPa of membrane B

The permeate showed more than 1.7 unit of purity rise, 78.6% reduction in turbidity and 28.94% reduction in colour as shown in Table 4 and Table 5. From the three runs, it can be seen that the permeate of membrane B is more in purity, percentage reduction of turbidity and percentage reduction of colour comparing to membrane A. Thus, membrane B gives purity clarified sugar cane juice.

Table.4.2 Comparison of juice properties at different flux at 300KPa of membrane A (without kaolin)

°Brix	TMP (kPa)	Temperature (°C)	Flux (litre/m² sec)	Decolorization (%)	Turbidity
16.29	300	25	942.23	24.99	900
16.26	300	25	393.5	23.68	950
16.30	300	25	341.15	21.05	980

Table.4.3 Comparison of juice properties at different flux at 300KPa of membrane B (with kaolin)

°Brix	TMP (kPa)	Temperature (°C)	Flux (litre/m² sec)	Decolorization (%)	Turbidity
16.31	300	25	245.126	26.315	460
16.30	300	25	50.18	27.63	490
16.28	300	25	35.60	28.94	500

4.7.2 Separation of crude oil from crude oil-water emulsion.

Crude oil water emulsion system prepared following the procedure described earlier (See Section 3.8.1). A brief overview of results on rejection of crude oil is summarized in the Table 6Here; we report a rejection percentage of approximately 52.32 % for crude from oil-water emulsion system. As indicated, cumulative rejection % increases as time of process increases. This is mainly attributed to blockage of larger pores by oil emulsion and formation of oil slick. Blockage of pores by the oil slick also causes increase in pressure drop across the membrane. However, higher operating pressure is not recommended for this micro-filtration system. Literature also reports the gradual reduction of flux with an increased oil concentration [10]. This is due to increase in the adsorptive and concentration polarization resistances because of higher feed concentration.

Table.4.4 Summary of crude oil-water emulsion separation using membrane B

Sl. No	Volume of Permeate (m ³)	Time Taken (Sec)	Area of Membrane (m ²)	Flux (m ³ m ⁻² s ⁻¹)	Rejection %
1	1×10 ⁻⁵	752.14	0.002317	5.59424×10 ⁻⁰⁶	32.23
2	2×10 ⁻⁵	915.6	0.002317	9.1942×10 ⁻⁰⁶	36.83
3	3×10 ⁻⁵	1169.4	0.002317	1.07998×10 ⁻⁰⁶	40.23
4	4×10 ⁻⁵	1524.6	0.002317	1.1623×10 ⁻⁰⁶	52.32

We also observed that size of oil droplet and initial oil concentration in the emulsion system is also an important factor that determines the rejection percentage. An increase in oil rejection up to 85% with simultaneous decrease in flux is reported elsewhere [10] However for the operating pressure of 300 kPa, they obtained rejection of 44 % (This work reports a rejection of 52.32 % for 275 kPa). The coalescence and wetting of oil droplets with increased pressure force oil drops through the membrane pores is the reason for decreased rejection percentage.

4.8 Estimation of material cost of the membrane

The material cost of the solvothermally fabricated membrane is calculated in terms of Rupees per square meter. 42gms of clay has been taken in addition with the other materials in their respective composition as described in Ref.1. From this total 04 supports are fabricated. Diameter and thickness of each sample has been measured using vernier calliper. Total surface area of each sample was calculated assuming them cylindrical in shape. The purchasing cost of each chemical in rupees per gram was known. From this material cost of the required chemicals can be determined. Dividing this cost with total surface area of sample prepared we can get the material cost for fabrication of ceramic membrane in rupees per square meter.

Table.4.5 Materials used with their cost for membrane A

Name of the material	Cost (rupees/gram or ml)	Amount required (gm or ml)	Total cost (rupees)
Clay	-	29	-
Water	-	8	-
Sodium carbonate (MERCK)	0.432	2.5	1.08
Sodium meta silicate (LobaChemie)	0.644	1.4	0.9016
Boric acid (RANKEM)	0.9	1.1	0.99
Total			2.9716

Table.4.6 Materials used with their cost for membrane B

Name of the material	Cost (rupees/gram or ml)	Amount required (gm or ml)	Total cost (rupees)
Clay	-	28	-
Kaolin	0.46	8	3.68
Water	-	10	-
Sodium carbonate (MERCK)	0.432	2	1.08
Sodium meta silicate (LobaChemie)	0.644	1	0.9016
Boric acid (RANKEM)	0.9	1	0.99
Total			6.6516

The total materials cost per unit area is **534 & 1185.67 rupees per square meter** for the fabrication of membrane A & B Respectively.

Microfiltration membranes A were prepared from red mud with the addition of a small amount of sodium carbonate, sodium metasilicate and boric acid, membrane B is prepared with addition of kaolin. This study indicates that a defect-free ceramic membrane can be fabricated with high content of red mud and low content of expensive precursors. The thermal characterization and XRD study inferred that the appropriate sintering temperature for the chosen composition of membrane is 800°C for membrane A and Membrane B. The observable maximum pore size of the membrane A is 10µm and for the membrane B is 6µm. the distribution of pore size based on SEM and physical interpretation is good and only 18.85-16.52% of porous structure contribution towards the transport studies and from the Mercury porosimetry analysis the porosity of the membrane A & B is 18.852 & 24.26% respectively. These results provide significant opportunity to develop ceramic micro-filtration membranes with flexible pore sizes for industrial application. The surface area of the ceramic membrane A is 219.19 m²/gm by BET surface analyzer.

The performance of ceramic membranes A and membrane B in clarifying sugar cane juice was investigated 300 kPa TMP. For a membrane A the average flux will be 558.96 liter/m² hr. and for membrane B 110.302 liter/m²hr and percentage decolonization will be 24.94 and 28.94% respectively. Separation of crude oil from crude oil-water emulsion using membrane B is 53.23 (% Rejection).

The approximate cost of the membrane fabricated is cheaper than commercially available ceramic membranes and compare well with other reported cost data. These results provide significant opportunity to develop ceramic micro-filtration membranes with flexible pore sizes for industrial application.

REFERENCES

- 1) Chuan-shengWu and Dong-yan Liu “Mineral Phase and Physical Properties of RedMudCalcined at Different Temperatures”*Hindawi Publishing Corporation Journal of Nanomaterials Volume 2012, Article ID 628592.*
- 2) Ping Wang and Dong-Yan Liu “Physical and Chemical Properties of Sintering Red Mud and Bayer Red Mud and the Implications for Beneficial Utilization” *Materials* 2012, 5, 1800-1810; doi:10.3390/ma5101800.
- 3) Richard W. Baker “Membrane technology and applications” 2nd Editions *Membrane Technology and Research, Inc. Menlo Park, California.*
- 4) M. Hamachi, B.B. Gupta, R. Ben Aim “Ultrafiltration: a means for decolorization of cane sugar solution” *Separation and Purification Technology* 30 (2003) 229-239.
- 5) B. Farmani, J. Hesari, S. Aharizad “Determining Optimum Conditions for Sugarcane Juice Refinement by Pilot Plant Dead-end Ceramic Micro-filtration” *J. Agric. Sci. Technol.* (2008) Vol. 10: 351-357.
- 6) V. Jegatheesana,D.D. Phonga,L. Shua, R. Ben Aim “Performance of ceramic micro- and ultrafiltration membranes treating limed and partially clarified sugar cane juice” *Journal of Membrane Science* 327 (2009) 69–77.
- 7) R.J. Steindl and D.W. Rackemann “Membrane filtration of clarified juice” *Proc. Int. Soc. Sugar Cane Technol., Vol. 27, 2010.*
- 8)V. Jegatheesan, L. Shu, G. Keir, D. D. Phong “Evaluating membrane technology for clarification of sugarcane juice” *Rev Environ SciBiotechnol* (2012) 11:109–124.
- 9) A.M. Ghosh, M. Balakrishnan “Pilot demonstration of sugarcane juice ultrafiltration in an Indian sugar factory” *Journal of Food Engineering* 58 (2003) 143–150.

- 10) M.J. Um, S.H. Yoon, C.H. Lee, K.Y. Chung, K.Y. Kim, "Flux enhancement with gas injection in crossflow ultrafiltration of oily wastewater" *Water Res.* 35 (2001) 4095–4101.
- 11) A. El-Kayar, M. Hussein, "Removal of oil from stable oil-water emulsion by induced air floatation technique" *Sep. Technol.* 3 (1993) 25–31.
- 12) A.Y. Hosny, "Separating oil from oil-water emulsions by electroflotation technique" *Sep. Technol.* 6 (1996) 9–1.7
- 13) J. Cui, X. Zhang, H. Liu, "Preparation and application of zeolite/ceramic microfiltration membranes for treatment of oil contaminated water" *J. Membr. Sci.* 325 (2008) 420–426.
- 14) B.K. Nandi, A. Moparthy, "Treatment of oily wastewater using low cost ceramic membrane: comparative assessment of pore blocking and artificial neural network models" *Chem. Eng. Res. Des.* 88 (2010) 881–892.
- 15) D. Vasanth G. Pugazhenth, R. Uppaluri "Fabrication and properties of low cost ceramic microfiltration membranes for separation of oil and bacteria from its solution" *J. Membr. Sci.* 379 (2011) 154– 163.
- 16) B. Chakrabarty, A.K. Ghoshal, M.K. Purkait "Ultrafiltration of stable oil-in-water emulsion by polysulfone membrane" *J. Membr. Sci.* 325 (2008) 427–43.7
- 17) S. Jana, M.K. Purkait, K. Mohanty, "Preparation and characterization of low-cost ceramic microfiltration membranes for the removal of chromate from aqueous solutions" *Appl. Clay Sci.* 47 (2010) 317-324.
- 18) S. Jana, A. Saikia, M.K. Purkait "Chitosan base ceramic ultrafiltration membrane: preparation, characterization and application to remove Hg(II) and As(III) using polymer enhanced" *Chem. Eng. Journal* 170 (2011) 209-219.
- 19) V. Jegatheesan, L. Shu, G. Keir, D. D. Phong "Evaluating membrane technology for clarification of sugarcane juice" *Rev Environ Sci Biotechnol* (2012) 11:109–124.

- 20) R.J. Steindl and D.W. Rackemann “Membrane filtration of clarified juice” *Proc. Int. Soc. Sugar Cane Technol.*, Vol. 27, 2010.
- 21) G. C. Gonçalves, E. S. Mendes, N. C. Pereira “Operating parameters influence of ultrafiltration on flux and quality of sugarcane juice permeate” *2nd Mercosur Congress on Chemical Engineering*.
- 22) A.M. Ghosh, M. Balakrishnan “Pilot demonstration of sugarcane juice ultrafiltration in an Indian sugar factory” *J. of Food Engg.* 58 (2003) 143–150.
- 23) Balakrishnan, M., Dua, M., & Bhagat, J. J. “Effect of operating parameters on sugarcane juice ultrafiltration: results of a field experience” *Separation and Purification Technology*, 19, 209–220.
- 24) Balakrishnan, M., Dua, M., & Bhagat, J. J. “Evaluation of ultrafiltration for juice purification in plantation white sugar manufacture” *International Sugar Journal*, 1213, 21–24
- 25) Balakrishnan, M., Dua, M., & Khairnar, P. N. “Significance of membrane type and feed stream in the ultrafiltration of sugarcane juice” *Separation Science and Technology*, 36(4), 619–637.
- 26) Bhattacharya, P. K., Agarwal, S., De, S., & Rama Gopal, U. V. S. “Ultrafiltration of sugar cane juice for recovery of sugar: analysis of flux and retention” *Separation and Purification Technology*, 21, 247–259.
- 27) Y. Yoshino, T. Suzuki, B.N. Nair, “Development of tubular substrates, silica based membranes and membrane modules for hydrogen separation at high temperature” *J. Membr. Sci.* 267 (2005) 8–17.
- 28) G. Pugazhenthiraj, S. Sachan, N. Kishore, “Separation of chromium (VI) using modified ultrafiltration charged carbon membrane and its mathematical modelling” *J. Membr. Sci.* 254 (2005) 229–239.
- 29) J.M. Benito, A. Conesa, F. Rubio, “Preparation and characterization of tubular ceramic membranes for treatment of oil emulsions” *J. Eur. Ceram. Soc.* 25 (2005) 1895–1903.
- 30) D.S. Bae, D.S. Cheong, K.S. Han, “Fabrication and microstructure of Al_2O_3 – TiO_2 composite membranes with ultrafine pores” *Ceram. Int.* 24 (1998) 25–30.

- 31) K.A. DeFriend, M.R. Wiesner, A.R. Barron, "Alumina and aluminate ultrafiltration membranes derived from alumina nanoparticles" *J. Membr. Sci.* 224(2003) 11–28.
- 32) W. Zeng, L. Goa, L. Gui, J. Guo, "Sintering kinetics of α -Al₂O₃" *Ceram. Int.* 25 (1999) 723–726.
- 33) N. Saffaj, M. Persin, S.A. Younssi, "Labot, Removal of salts and dyes by low ZnAl₂O₄–TiO₂ ultra-filtration membrane deposited on support made from raw clay" *Sep. Purif. Technol.* 47 (2005) 36–42.

Research publications

International conference

- **Sandeep Parma**, Sankaranarayanan Hariharan, and Pradip Chowdhury “Preparation and Characterization of Ceramic Membranes from Red Mud” *International Conference on Sustainable Technologies for Energy and Environment in Process industries. CHEMCON-2012. NIT Jalandhar*